

1 **A comprehensive review on biopolymer mediated nanomaterial composites and**
2 **their applications in electrochemical sensors.**

3
4 *Mugashini Vasudevan^{1,2}, Veeradasan Perumal^{1,2,*}, Saravanan Karuppanan², Mark Ovinis³,*
5 *Pandian Bothi Raj^{4,**}, Subash C.B. Gopinath⁵, and Thomas Nesakumar Jebakumar Immanuel*
6 *Edison⁶*

7
8 *¹Centre of Innovative Nanostructures and Nanodevices (COINN), Universiti Teknologi*
9 *PETRONAS, 32610 Seri Iskandar, Perak Darul Ridzuan, Malaysia*

10 *²Department of Mechanical Engineering, Universiti Teknologi PETRONAS, 32610 Seri Iskandar,*
11 *Perak Darul Ridzuan, Malaysia.*

12 *³School of Engineering and the Built Environment, Birmingham City University, B4 7XG, UK*

13 *⁴School of Chemical Sciences, Universiti Sains Malaysia, 11800, Penang, Malaysia*

14 *⁵Institute of Nano Electronic Engineer, Kangar 01000 & Faculty of Chemical Engineering*
15 *Technology, Arau 02600, Universiti Malaysia Perlis, Perlis, Malaysia*

16 *⁶School of Chemical Engineering, Yeungnam University, Gyeongsan, Gyeongbuk 38541, Republic*
17 *of Korea*

18

19

20

21

22

23

24

25

26

27 **Corresponding email: veeradasan.perumal@utp.edu.my*

28 **Corresponding phone number: +6010-377374*

29 ***Corresponding email: bothiraja@gmail.com*

30 ***Corresponding phone number: +6016-7859243*

31

Abstract

32
33
34
35
36
37
38
39
40
41
42
43
44
45
46
47
48
49
50
51
52
53
54
55
56
57
58
59

Biopolymers are an attractive green alternative to conventional polymers, owing to their excellent biocompatibility and biodegradability. However, their amorphous and nonconductive nature limits their potential as active biosensor material/substrate. To enhance their bio-analytical performance, biopolymers are combined with conductive materials to improve their physical and chemical characteristics. We review the main advances in the field of electrochemical biosensors, specifically the structure, approach, and application of biopolymers, as well as their conjugation with conductive nanomaterials, polymers, and metal oxides in green-based non-invasive analytical biosensors. In addition, we reviewed signal measurement, substrate bio-functionality, biochemical reaction, sensitivity, and limit of detection (LOD) of different biopolymers on various transducers. To date, pectin biopolymer, when conjugated with either gold nanoparticles, polypyrrole, reduced graphene oxide, or multiwall carbon nanotubes forming nanocomposites on glass carbon electrode transducer, tends to give the best LOD, highest sensitivity, and can detect multiple analytes/targets. This review will spur new possibilities for the use of biosensors for medical diagnostic tests.

Keywords: Biopolymers; Nanosensors; Sensing elements; high-performance detection

Contents

60	1.	Introduction.....	3
61	2.	Biopolymer synthesis, structure and physical properties.....	6
62		2.1 Cellulose.....	6
63		2.2 Chitosan.....	7
64		2.3 Lignin.....	9
65		2.4 Starch.....	10
66		2.5 Pectin.....	11
67	3.	Biopolymer with nanoparticles composite based electrochemical sensor.....	11
68		3.1 Biopolymer-silver nanoparticles (Ag NPs).....	12
69		3.2 Biopolymer-gold nanoparticles (Au NPs).....	13
70		3.3 Biopolymer-carbon nanoparticles (CNPs).....	14
71		3.4 Biopolymer-copper nanoparticles (Cu NPs).....	15
72		3.5 Biopolymer-double nanoparticles.....	16
73		3.6 Biopolymer-oxides nanoparticles.....	17
74		3.7 Biopolymer nanoparticles.....	17
75	4.	Biopolymer with polymers (conducting or synthetic) composites based electrochemical sensor.....	23
76		4.1 Biopolymer-polyaniline (PANI).....	23
77		4.2 Biopolymer-polypyrrole (PPy)	25
78		4.3 Biopolymer-poly(3,4-ethylenedioxythiophene) (PEDOT).....	27
79		4.4 Biopolymer-polyacrylonitrile (PAN).....	28
80		4.5 Biopolymer-polyurethanes	29
81	5.	Biopolymer with nanomaterial composite based electrochemical sensor.....	33
82		5.1 Biopolymer-metal oxides.....	33
83		5.2 Biopolymer-graphene.....	35
84		5.3 Biopolymer-molybdenum disulfide (MoS₂).....	36
85		5.4 Biopolymer-nanodiamonds.....	37
86	6.	Conclusion and future perspectives.....	41
87			
88			

89.0 Introduction

90 Electrochemical biosensors are simple devices that transform biochemical information
91 produced from a redox reaction into an electrical signal^[1]. They play an important role in detecting
92 biomarkers and monitoring environmental pollutants by detecting various bio-analytes and
93 compounds. Their ease of use, simplicity, high sensitivity, portability, low-cost, rapid response,
94 and eco-friendliness have led to their widespread adoption^[2, 3]. The performance of biosensors
95 depends on three main components, namely a bioreceptor, a transducer, and a signal processing
96 system. A bioreceptor comprises an immobilized biocomponent that can detect a specific analyte.

97 Examples of biocomponents include antibodies, nucleic acids, enzymes, cells, and biomarkers.
98 The interaction between a bioreceptor and an analyte results in chemical changes such as the
99 synthesis of a new chemical, heat release, electrons flow, and change in pH and mass. A transducer
100 or a converter converts the biochemical changes due to the interaction between the analyte and the
101 bioreceptor into an electrical signal. The electrical signal is subsequently amplified and processed
102 as a digital display, a print-out, or as an optical change. The layering of probe material on a
103 transducer increases the strength of the response signal in terms of its current, potential, or
104 impedance. The greater the stacking, the higher the signal strength. Various electrochemical
105 measurable techniques such as electrochemical impedance spectroscopy (EIS), differential pulse
106 voltammetry (DPV), linear sweep voltammetry (LSV), cyclic voltammetry (CV), anodic stripping
107 voltammetry (ASV), differential pulse stripping voltammetry (DPSV), differential pulse anodic
108 stripping voltammetry (DPSAV), square wave anodic stripping voltammetry (SWASV) and
109 square wave voltammetry (SWV) have been used to measure the interaction between analyte and
110 target. When an analyte/target and electrode interact, there is a measurable change in current and
111 potential of a biosensor, depending on the target/analyte concentration on the sensing surface of
112 the electrode.

113 There are three types of electrodes used in electrochemical sensing, a working electrode, a
114 counter or auxiliary electrode, and a reference electrode^[4]. For reliable measurement, the stability
115 of these electrodes is crucial, especially in terms of conductivity and chemical composition. The
116 working or sensing electrode acts as a transducer during the interaction of the bioreceptor and
117 analyte/target, while the counter electrode measures the current flow to and from the sensing
118 electrode and forms a connection path between the electrode surface and electrolyte solution. The
119 reference electrode, commonly silver chloride, provides a stable potential when placed at a
120 constant distance from the working electrode^[5]. Electrochemical biosensors that function using a
121 liquid medium are generally classified based on the type of measurement, as well as depending on
122 the type of transducer (electrode) used, such as amperometric (current), potentiometric (potential),
123 impedimetric (impedance) and conductometric (modifying conductive properties of a medium)<sup>[6-
124 9]</sup>.

125 Chemical modification of these electrodes can enhance its electrochemical sensing properties.
126 The electrodes are usually modified with toxic non-biodegradable active materials such as carbon-

127 derivatives and synthetic polymers. Recently, biopolymers have emerged as a promising
128 environmentally friendly alternative to synthetic polymers as a polymer host in electrolytes.
129 Biopolymers are polymers that are derived from living matter and can be grouped into three types,
130 namely natural, synthetic, and microbial. Natural biopolymers are macromolecules that are
131 extracted from natural sources, while synthetic biopolymers are derived from biological precursor
132 materials, whereas microbial biopolymers are produced by organisms such as algae, bacteria, and
133 fungi from carbon^[10]. Common natural biopolymers are polysaccharides, polyester, and protein,
134 which are found in plants and animals and are composed of numerous amino acids and nucleotides
135 that form a large structure from linear chains that are bonded covalently.

136 Biopolymers are environmentally friendly, biocompatible, biodegradable, flexible,
137 inexpensive, and form easily. Owing to their abundance and diverse structures, biopolymers have
138 been extensively used in biomedical^[11], supercapacitors^[12], biosensors^[13], drug delivery, tissue
139 engineering, and environment monitoring^[14] applications. The most widely used biopolymers are
140 polysaccharides such as cellulose, chitosan, lignin, starch, and pectin, as these biopolymers can be
141 easily modified and functionalized owing to their diverse chemical composition, numerous
142 reactive sites, and remarkable structural features^[15,16]. The main functions of biopolymers in
143 electrochemical sensors are for biochemical modification, to induce bio-functionality,
144 conductivity, and biochemical reaction. However, biopolymers have poor solubility, high thermal
145 degradability, high chemical degradability, and poor mechanical properties. Nevertheless, these
146 limitations can be mitigated with conductive additives such as nanoparticles, conducting polymers,
147 and metal oxides. These combinations are mostly environment friendly compared with non-
148 biopolymer alternatives such as graphene or graphene oxide, which require lengthy processing
149 time and hazardous chemicals.

150 The solubility properties of biopolymers are based on the strength of hydrogen bonds in
151 intramolecular or intermolecular interactions. Generally, weak hydrogen bond interactions with
152 amino groups facilitate the dissolution of biopolymers in common organic and diluted aqueous
153 solvents. The existence of amino groups affects the pH of the solvent, changing the charge state
154 and accountabilities of biopolymers. The ease of dissolving biopolymers in ordinary solvents
155 makes its processing and chemical modification feasible. The biodegradability and solubility of
156 biopolymers are principally attributed to their vulnerability to biomolecules such as enzymes,

157 proteins, and body tissues. Therefore, modification of biopolymers with both inorganic and organic
158 materials is required. For example, the electrical conduction of a biopolymer can be further
159 enhanced with conductive materials and modifying its hydroxyl, carboxyl, and amino groups^{[17–}
160 ^{19]}. These modified biopolymer composites acquire useful properties from the added material while
161 retaining the advantages of the biopolymers^[20]. As for sensing applications, the immobilizing
162 properties in biopolymers and their compatibility with bodily fluids make biopolymers an ideal
163 biosensor candidate.

164 There is growing interest in conjugating biopolymers such as cellulose, chitosan, lignin, starch,
165 and pectin with supporting materials such as nanoparticles, conducting polymers, and metals for
166 electrochemical sensors (Figure 1). To the best of our knowledge, there is no comparative study
167 yet on biopolymers such as cellulose, chitosan, lignin, starch, and pectin composites in terms of
168 signal measurement, substrate bio-functionality, biochemical reaction, sensitivity, and limit of
169 detection. In this review, the applicability of biopolymers as a stabilizer and a reducing agent is
170 reviewed, with emphasis on the synthesis, structure, and physical development of biosensors.
171 Pectin biopolymer, when combined with gold nanoparticles, polypyrrole, reduced graphene oxide,
172 or multiwall carbon nanotubes on a glass carbon electrode transducer, tends to give the best limit
173 of detection (LOD), highest sensitivity, and can detect multiple analytes/targets compared to other
174 biopolymers considered. This review also summarizes the various types of biopolymer composites
175 available and their applicability for medical diagnostic tests.

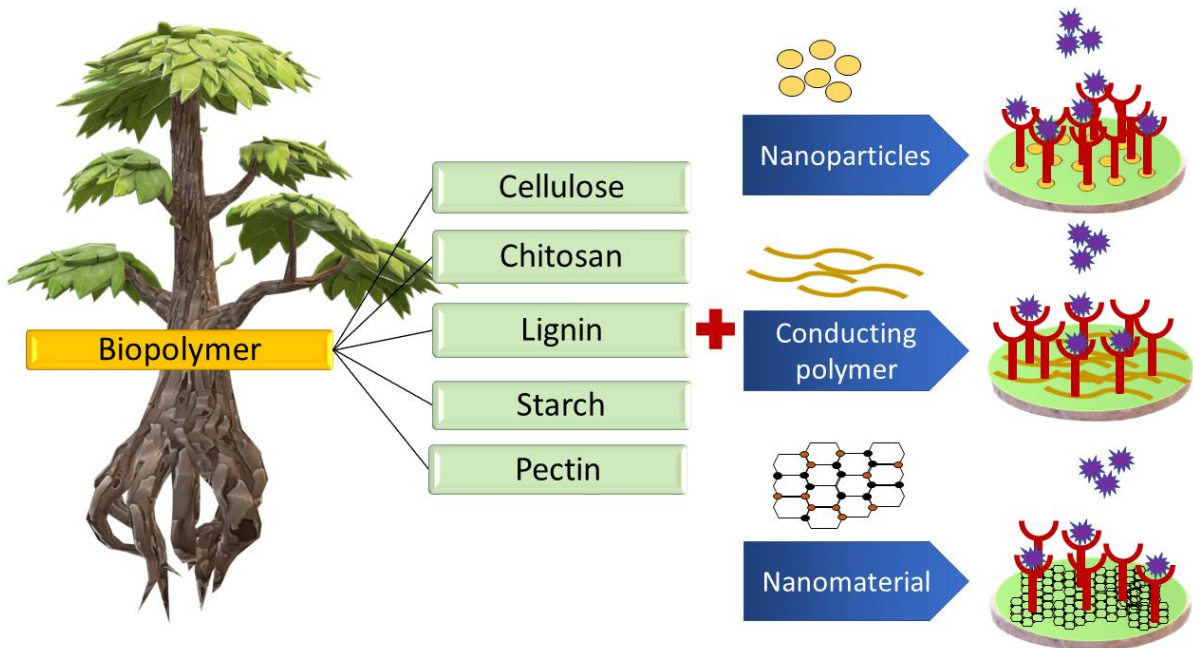


Figure 1: Schematic illustration of biopolymer conjugate with nanoparticles, conducting polymer, and nanomaterial in electrochemical sensors.

176
177
178
179

182.0 Biopolymer synthesis, structure, and physical properties

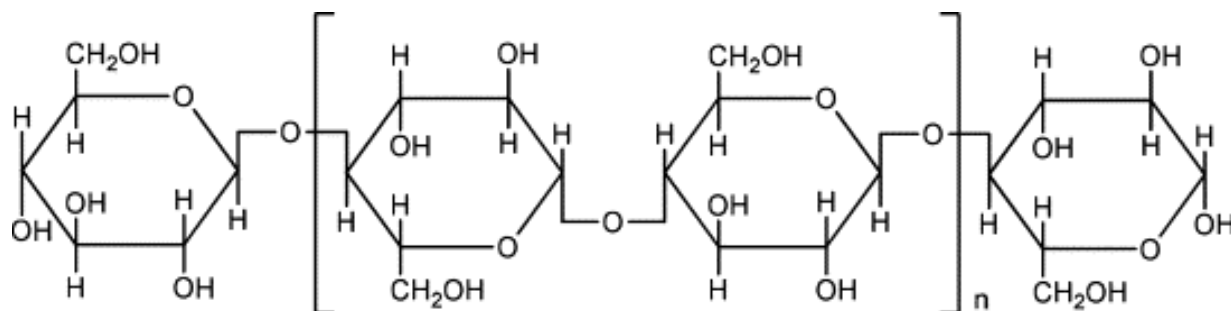
181 Biopolymers such as cellulose, chitosan, lignin, starch, and pectin have different chemical
182 and physical properties, as well as structures. The oxygen-rich polysaccharide of cellulose and
183 starch provides good mechanical strength and acts as a reducing agent, whereas chitosan, with its
184 dual-skeleton structure, can maintain its original features even after alteration to its structure.
185 Lignin is the only biopolymer that can form a polyaromatic structure via an acetylation process.
186 Pectin, made of a sugar compound, has biodegradable stabilizer properties that can easily capture
187 covalently bonded biomaterials. These biopolymers have unique properties, such as
188 crystallization, high toughness, oxygen permeability, carbon content, and being a reducing and
189 stabilizing agent. A detail description of these biopolymers is given below.

190 2.1 Cellulose

191 Cellulose is one of the most popular polysaccharides used in biosensors. An abundant
192 biopolymer, it is an oxygen-rich polysaccharide composed of an anhydroglucose unit bonded by
193 an oxygen linkage^[21]. Cellulose is generally synthesized by plants, but it is also formed through
194 bacterial interactions^[22]. It is tough and fibrous, important in preventing plant cell walls from

195 collapsing. Cellulose has the highest strength of all biopolymers, due to its chains that are
196 organized in fibrils, which enables the formation of a bundle of polysaccharides cell wall. It has
197 both a crystalline and an amorphous nature, as shown in Figure 2, which can be observed from its
198 carbon atoms compositions. However, it is these very characteristics that prevent its use as an
199 active biosensor material, due to its poor electrical conductivity and extreme hydrophilicity.
200 Hence, the cellulose structure must be modified chemically and physically.

201 Cellulose can be modified to form porous surface cellulose nanofibers (CNFs), high absorption
202 capacity cellulose nanocrystals (CNCs), and conductive carboxymethyl cellulose (CMC). CNFs
203 are made of β -1,4 linked anhydro-D-Glucose unit and are excellent for biosensing applications, as
204 it has a large surface area, porous structure, and abundant hydroxyl groups, which act as binding
205 sites for analyte biomarkers. CNFs can be electrospun to maintain a width of 5 to 20 μ [23]. The
206 porous surface of CNFs can be tailored by controlling parameters such as precursor ratio, voltage,
207 solution viscosity, rotational drum speed, relative humidity, and distance between needle and drum
208 during electrospinning. Acid hydrolysis is used to convert crystalline cellulose to CNCs.
209 Hydrolyzed CNCs are non-cytotoxic, resistant to oxidative stress, highly biocompatible, and
210 extensively used in biomedical industries and electronic applications^[24]. Additionally, CNCs have
211 a large aspect ratio, good mechanical properties, low thermal-expansion, and high biomolecule
212 absorption capacity. CNCs can be easily modified through hydrolysis and oxidation to form
213 carboxylated CNCs, which are rich in carboxyl and hydroxyl groups that bind nanoparticles firmly,
214 owing to their strong ability to adsorb nanoparticles. Furthermore, both CNFs and CNCs have
215 excellent polymer composite stability in water, owing to the electron-rich properties of hydroxyl
216 and sulfate ester groups on their surface. On the other hand, CMCs are composed of carboxymethyl
217 groups ($-\text{CH}_2\text{COO}^-\text{Na}^+$) that are bound to the cellulose backbone that exchanges its sodium ions
218 with various metal ions. It also has numerous $-\text{COOH}$ and $-\text{OH}$ functional groups in its polymer
219 structure, which gives it hydrophilic properties and forms coordination bonds with metal ions. The
220 conductivity of CMC as a polyelectrolyte makes it ideal for the detection of heavy metal ions^[25].
221 All these nano-cellulosic materials, which are negatively charged, react with positively charged
222 materials to form electrostatic interactions that enhance the mechanical properties and
223 dispersibility of the biomaterials, which in turn improves the selectivity of biosensors ^[26, 27].



224

225 **Figure 2:** (a) Repeating unit of cellulose, (b) the crystalline and amorphous regions of cellulose
 226 chains. Reproduced with permission from Ref.^[28] Copyright 2015, Elsevier

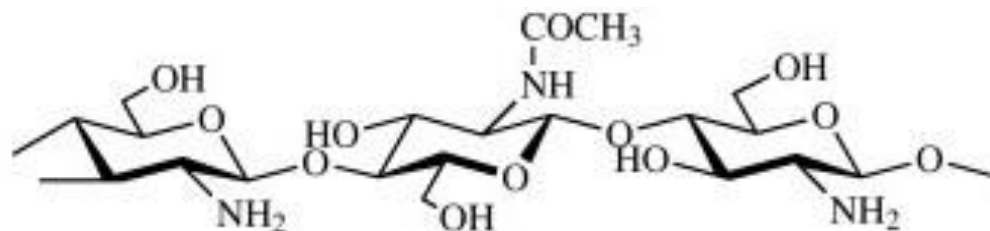
227

228 2.2 Chitosan

229 Chitosan is a biopolymer that forms from the deacetylation of chitin and has both an
 230 exoskeleton and endoskeleton structure^[29]. Chitosan comprises linear polysaccharide chains
 231 consisting of D-glucosamine and N-acetyl-D-glucosamine bonded by glycosidic^[30, 31], as shown
 232 in Figure 3. The structures of chitin and chitosan are markedly different, as observed by the
 233 acetamide and amine structures in chitin and chitosan respectively. The free amine groups in
 234 chitosan are active sites for chemical reactions, which is especially useful in modifying chitosan
 235 into composites. The amine group in chitosan is the reason for its widespread use in various
 236 applications such as the food industry, biomedical, biosensors, waste water treatment, and
 237 environmental monitoring^[32]. The properties of chitosan depend on the degree of deacetylation
 238 (DDA) and molar mass^[33]. Chitosan has an average DDA of 80 %, whereas chitin has an average
 239 DDA below 50 %. Chitosan can be categorized as chitosan I with low DDA and chitosan II with
 240 high DDA. The functionality of chitosan is mostly dependent on the pH of the solution. High
 241 DDA (> 50 %) enables chitosan to be dissolved in diluted acidic solutions. The amines in chitosan
 242 become positively charged between a pH of 3 to 4, but remain insoluble, as it is unable to attract
 243 hydrogen atoms from the solution to form a positively charged amine group^[34]. The protonated
 244 amine group in acid solution attracts chitosan, which reacts with negatively charged biomolecules
 245 or structures. The glycosidic bond in chitosan is a type of covalent bond that joins a carbohydrate
 246 molecule to another functional group. The glycosidic bond in chitosan helps in the formation of
 247 chitosan film or membranes, which is an excellent biosensor surface immobilization matrix^[35].
 248 Structural or physical alteration of chitosan chemically does not change its original properties. It
 249 can retain its non-toxic, biodegradable, biocompatible, and minimal immunogenic properties while

250 reacting with additive organic/inorganic material because of the presence of hydroxyl and amine
251 groups ^[36]. It can be re-shaped and re-sized into sol-gels, nanofibers, and nanoparticles. Since it is
252 nonconductive, its electrical properties have to be enhanced by the addition of conductive material
253 such as gold nanoparticles ^[37], conducting polymer such as polypyrrole^[38] and polyaniline^[39], as
254 well as metal oxide such as manganese (IV) oxide^[40].

255



Chitosan

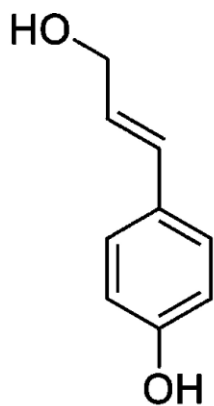
256

257 **Figure 3:** Structure of chitosan constituting co-polymer of glucosamine and acetyl-glucosamine.
258 Reproduced with permission from Ref ^[41] Copyrights 2012, Elsevier.

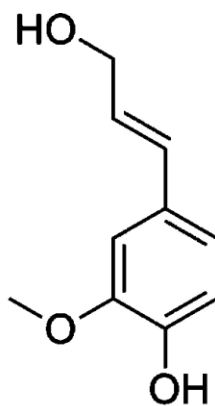
259 2.3 Lignin

260 Lignin is the second most abundant biopolymer after cellulose that can be extracted from
261 wood, paper, and pulp. In lignocellulose, lignin is responsible for binding cellulose and
262 hemicellulose. Lignocellulosic plants and animals (crustaceans) derived biomass is made up of 40-
263 50% cellulose, hemicellulose composed of 15-30% polysaccharides, and aromatic polymer
264 consisting of N-acetyl polysaccharides^[42]. The strong hydrophobicity of lignin present in the
265 secondary cell wall of lignocellulosic plants keeps the plant from collapsing and decaying, as lignin
266 enhances the mechanical support and water transportation system through the xylem in the bark of
267 a plant. Lignin has a three-dimensional amorphous network and it is a bio-renewable resource that
268 generates aromatic biochemical^[43]. Moreover, lignin is the only poly-aromatic structured
269 biopolymer in plants that is composed of three types of phenyl-propane monomers, namely
270 coniferyl alcohol, sinapyl alcohol and p-coumaryl alcohol, which forms the structured backbone
271 of lignin, as shown in Figure 4. The reactivity, environmental impact, and degree of branching of
272 lignin are based on the proportions of these three types of monomers in lignin. The flexible
273 monomers can be broken down into three phenolic sub-structures, namely guaiacyl (G), syringyl
274 (S), and p-hydroxyphenyl (H) units. These sub-structures consist of numerous functional groups
275 such as hydroxyls, carboxyls, carbonyls, and methoxyls that are widely utilized as active sites in
276 electrochemical biosensing. The composition of many functional groups makes lignin a high-value
277 functional material due to its high molecular weight, biocompatibility, and sensitivity to
278 biomolecule interactions. Furthermore, the cross-linked flexible aromatic compound and
279 polyphenolic characteristics of lignin can be modified chemically and physically with
280 organic/inorganic material, making it ideal for the synthesis of a renewable bio-based sensing
281 platform. Acetylation of aliphatic and phenolic alcohol enhances the functionality of lignin, by
282 producing more hydrocarbons that interact with various classes of solvents. However, as lignin
283 has a complex structure, an efficient and reliable hydrolysis method is required to break the bonds
284 in lignin structure, improve its solubility and create a homogenous mixture^[44]. Amorphous lignin
285 has poor electrical conductivity, with a detection limit of $0.28 \times 10^{-6} \text{ mol L}^{-1}$ within concentrations
286 ranging from 5×10^{-6} to $2 \times 10^{-4} \text{ mol L}^{-1}$ ^[45]. As such, lignin needs to be conjugated with other
287 materials to increase its effectiveness as a biosensing material.

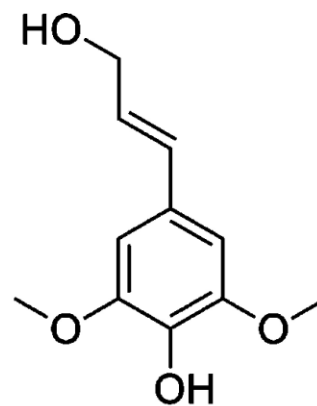
288



p-coumaryl alcohol



coniferyl alcohol



sinapyl alcohol

289

290

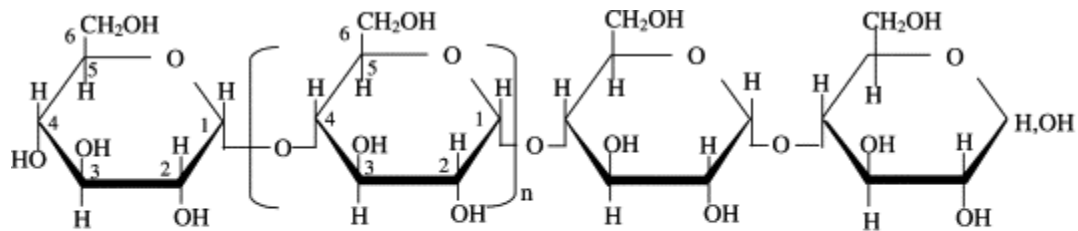
291

Figure 4: The three monolignols, the building block of lignin. Reprinted with permission from [46]. Copyright 2010, American Chemical Society

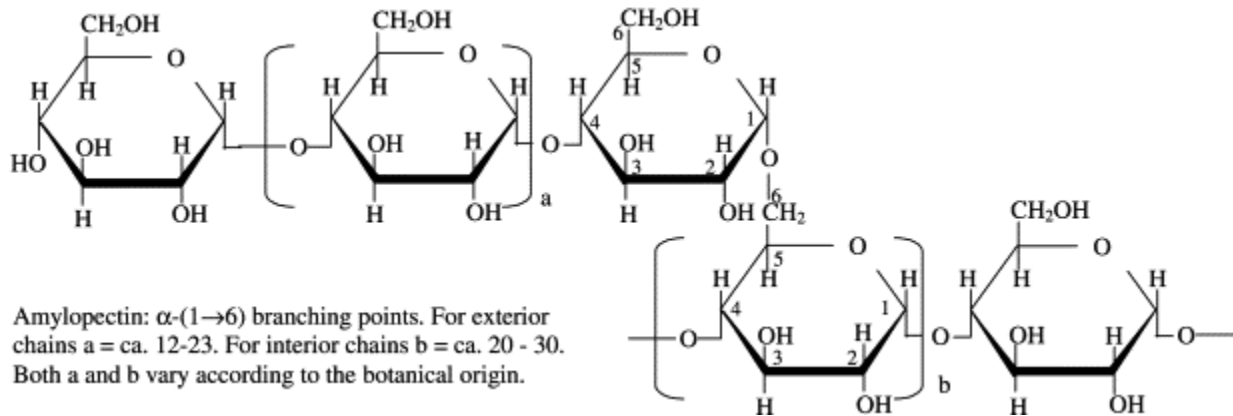
292 2.4 Starch

293 Starch is one of the largest carbohydrate polysaccharides composed of glucose monomers
294 bonded in α -1, 4-linkage and chain-shaped structure of amino acids (hydroxyl groups). The
295 structure can be reshaped and resized to easily form composites^[47, 48]. It can be commonly found
296 in the shape of spheres, platelets, and polygons with sizes ranging from 0.5 to 175 μm ^[49]. Raw
297 starch is available as granules and hydrolysis of these granules can break it down into nanowires
298 and nanoparticles with excellent electroactive properties. It can be classified as amorphous
299 (amylose) and crystalline (amylopectin) structures, as depicted in Figure 5. The insulated areas of
300 starch are composed of amylose chains and amylopectin branching points, whereas the semi-
301 crystalline areas of starch consist of amylopectin side chains with some of the amylose chains
302 having crystalline structures as well^[50]. Tatsumi et al.^[51] investigated the kinetics of hydrolyzed
303 starch by determining glucose levels from the glucoamylase deposition on various types of starch
304 granules surface namely, rice, wheat, maize, cassava, sweet potato, and potato. The number of
305 enzymes absorbed by each starch granule is influenced by the surface area, type, and crystalline
306 structure of the starch granules. They concluded that the density of the crystalline structure of
307 starch granules directly affects the amount of glucoamylase deposited on the surface of the starch
308 granules. Additionally, starch also functions as a cheap reducing agent and a chiral template for
309 one-dimensional structure formation. The large number of amyloses formed by the bonding with
310 the D-glucose unit in starch can reduce the complex structure of starch doped with foreign
311 molecules. Amylose is not active at room temperature and requires hydrothermal treatment for
312 structural modification of amylose branches to form crystalline structures, so that it can be used as
313 a template in the formation of hybrid nanoparticles and nanowires^[52]. Heat treatment of amylose
314 (starch) is a promising method to modify the structure in a simple, safe, and non-hazardous way.
315 However, starch exhibits poor electrical conductivity, low proton mobility, high sensitivity to
316 water and poor mechanical properties. In cold water, starch is somewhat susceptible to damage,
317 and in warm water, it produces starch hydrogels. To enhance the conductance and improve its
318 mechanical strength, starch is doped with conductive supporting material such as metal halides for
319 immobilization of bioreceptor and target^[53].

320



Amylose: α -(1 \rightarrow 4)-glucan; average $n = \text{ca. } 1000$. The linear molecule may carry a few occasional moderately long chains linked α -(1 \rightarrow 6).



Amylopectin: α -(1 \rightarrow 6) branching points. For exterior chains $a = \text{ca. } 12-23$. For interior chains $b = \text{ca. } 20 - 30$. Both a and b vary according to the botanical origin.

321

322 **Figure 5:** Structure of amylopectin and amylose in starch. Reused with permission from Ref. ^[54]

323

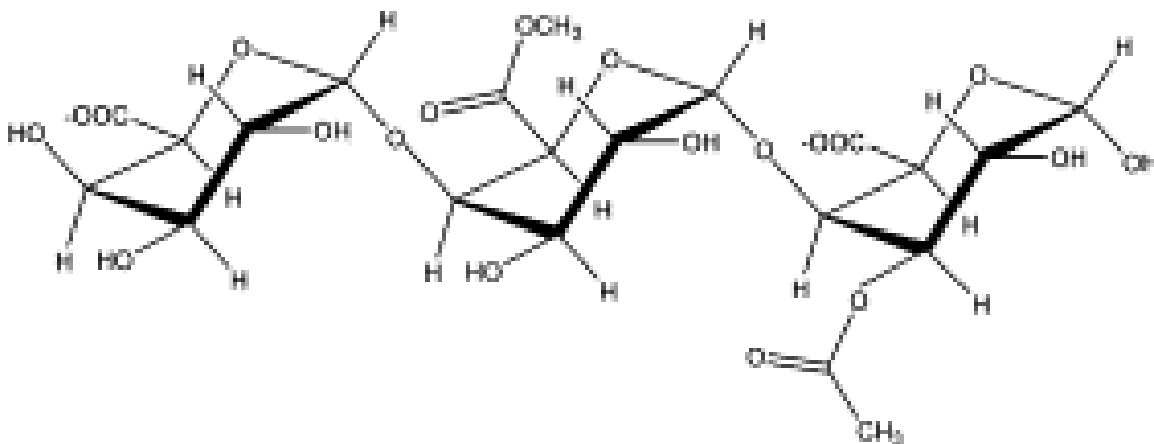
Copyright 2004, Elsevier

324

325 2.5 Pectin

326 Pectin or polygalacturonic acid is a naturally occurring polysaccharide with hydrophilic
327 properties that is suitable for stabilizing and immobilizing analytes on a sensing platform. Pectin
328 is primarily found in plant primary cell walls and skins of citrus fruits. It has methyl ester of (1-
329 4) α - D-galacturonic residues and rhamnogalacturonan that is partially attached to neutral sugars
330 namely, D-galactose, L-arabinose, D-xylose, L-fucose, and D-mannose^[55], as shown in Figure 6.
331 It has a linear anionic backbone with regions having no side chains known as “smooth regions”
332 and regions with non-ionic side chains known as “rough regions”. The high content of the sugar
333 compound makes pectin an attractive biodegradable alternative stabilizer, as pectin can be used to
334 trap covalently bonded enzymes and proteins on a sensing device. Pectin has abundant –OH and
335 –COOH functional groups that can be modified into various structures, especially to form gels and
336 films^[56]. The easily modified pectin can be combined with various substances to improve the
337 efficient transfer of analytes, as pectin has limited interfering electron chemical features^[57]. The
338 gelling features in negatively charged pectin form cross-linked pectin ‘egg box’ models, which
339 involve the formation of junction zones through electrostatic and ionic bonding interactions,
340 improving the sensitivity of biosensors^[58]. Calcium cross-linked pectin (CCLP) is an example of
341 ion cross-linked pectin network utilized as scaffolds for a stable hybrid material on a transducer
342 through simple and rapid electrodeposition processes^[59]. The free-moving calcium ions in calcium
343 react with the active sites of the hydroxyl and carboxyl group of pectin, forming CCLP. It has
344 maximum stability at pH 4, with degradation in terms of glycosidic linkage break down at low pH
345 and high temperature. In an alkaline solution, pectin de-esterifies and degrades at room
346 temperature^[60]. As pectin is an amorphous biopolymer, the addition of conductive materials is
347 necessary to improve the stability and conductivity of pectin-based materials. The coupling of
348 pectin with a carbon paste transducer is cost-effective for the determination of copper in biofuel,
349 with a detection limit of 2.5×10^{-8} mol L⁻¹ for a concentration range between 5.0×10^{-8} to $1.0 \times$
350 10^{-4} mol L⁻¹^[61]. Pectin can stabilize enzymes and proteins employed in bioactive layers, for
351 increased storage lifespan and reproducibility, as enzymes degrade at ambient temperature^[55].

352



353

354 **Figure 6:** Chemical structure of pectin. Reproduced with permission from Ref ^[62] Copyright
 355 2001, Elsevier

356.0 Biopolymer with nanoparticles composites in electrochemical sensor

357 Nanoparticles refer to small particles that have diameters between 1 and 100 nanometers. The
 358 shape and size depend entirely on its physical and chemical properties, and the fabrication method.
 359 Nanoparticles functions as immobilizer, signal amplifier, mediators, electroactive substances, and
 360 probe detection in biosensing applications. In recent years, there has been wide interest in
 361 nanoparticles-based biosensors because their flexible immobilization platform stabilizes
 362 biomolecules, enhances electron transportation, increases sensitivity and selectivity due to wide
 363 surface area, improves surface free energy and exhibits quantum phenomena. As such,
 364 biopolymer-nanoparticles composites have been frequently used because of their increased surface
 365 area, good electrical conductivity, reduced response time, good integration, adhesion, optical, and
 366 catalytic properties. Commonly used nanoparticles in biopolymer-nanoparticles composites are
 367 silver, gold, carbon, copper, and oxides. However, these nanoparticles have certain drawbacks
 368 namely, poor stability, poor reusability, and poor particle distribution^[38, 63]. Conjugation of
 369 biopolymers and nanoparticles can overcome these limitations.

370 3.1 Biopolymer-silver nanoparticles (Ag NPs)

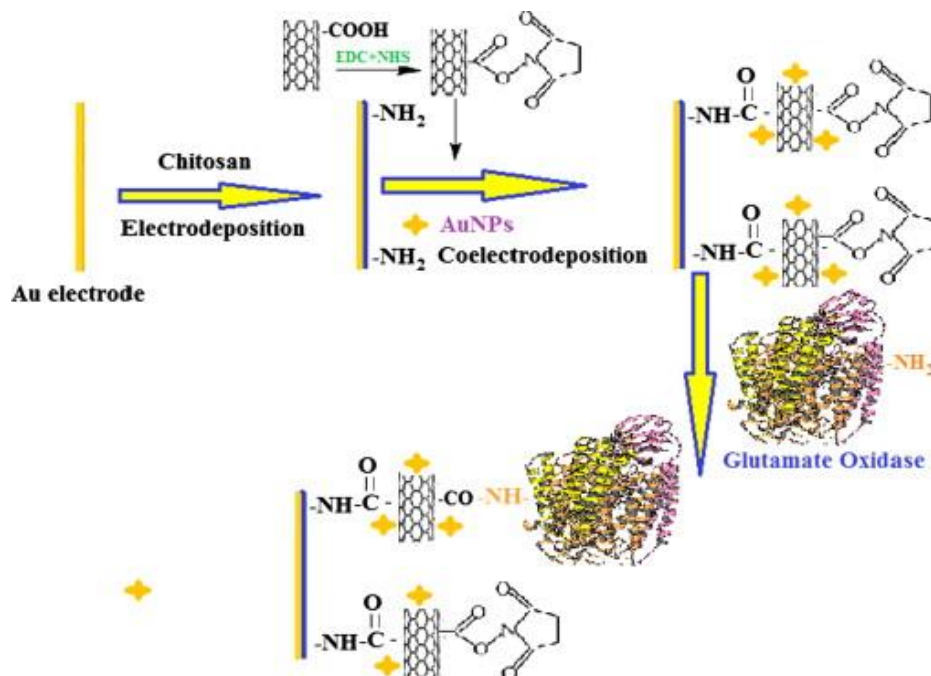
371 The porous polysaccharide chain in cellulose biopolymer helps in the deposition of
 372 nanoparticles. Liu et al.^[64] added Ag NPs on porous and high absorption capacity carboxylated
 373 CNC, forming a high-density surface area for the hybridization of target DNA on glass carbon
 374 electrodes (GCE). The CNC/AgNPs composites have a 2.3×10^{-11} mol L⁻¹ detection limit for a
 375 DNA concentration range of 1.0×10^{-11} to 1.0×10^{-7} mol L⁻¹. The CNC/Ag NPs were initially
 376 treated with sodium borohydride (NaBH₄) to reduce the metallic cation, to avoid interruption

377 during DNA detection. Apart from cellulose, chitosan and lignin react with Ag NPs because Ag
378 NPs are stable, have wide spectral features, and are easy to modify. The addition of chitosan with
379 Ag NPs improves the biocompatibility structure, nanoparticles aggregation, and adsorption
380 characteristics. P. Tiwari et al.^[65] developed a sensing probe from chitosan and Ag NPs to detect
381 azidothymidine on screen printed graphite electrode (SPGE) and glassy carbon electrode (GCE).
382 The biobased sensing probe has better azidothymidine detection on SPGE transducer with a
383 detection limit of 1 μM in buffer solution and 10 μM in biological samples (human plasma).
384 Saratale et al.^[44] synthesized a one-step method to embed silver Ag NPs in wheat straw lignin
385 through the ultrasonication method. A crystal-filled structure of phenolic, hydroxyl, and carboxylic
386 group in lignin-Ag NPs composite was produced. The lignin-Ag NPs composite reduces toxic
387 emissions to the environment and exhibits improved antimicrobial activity compared to metallic
388 Ag NPs in detecting hydrogen peroxide. Tai et al.^[66] reported on the use of oil palm lignin coupled
389 on a laser-scribed graphene nanofiber electrode for the rapid detection of tuberculosis (TB)
390 biomarker. This environmentally friendly and affordable sensing device with lignin-Ag NPs has
391 excellent binding, high electrical conductivity, low cytotoxicity, and remarkable analytical
392 performance. The lignin-Ag NPs form a string rigidly interconnected with single-strand DNA to
393 detect TB biomarkers, with a detection limit of 10^{-15} M using electrochemical impedance
394 spectroscopy (EIS). De Oliveira et al.^[67] synthesized starch-Ag NPs utilizing a mixture of silver
395 nitrate, soluble starch from potato, and sodium borohydride as a catalyst. They embedded starch-
396 stabilized Ag NPs on silsesquioxane polymer to detect triiodide, as silver forms a strong bond with
397 iodine. The protonated starch- Ag NPs bonded covalently to polycation silsesquioxane polymer,
398 using a layer-by-layer method on a fluorine-doped tin oxide substrate.

399 *3.2 Biopolymer-gold nanoparticles (Au NPs)*

400 Dong et al.^[68] used negatively charged gold nanoparticles (Au NPs) in developing a non-
401 enzymatic glucose sensor composed of poly(diallyldimethylammonium chloride)–cellulose
402 nanocrystal (PDDA–CNC)/Au NPs. The strong interaction of conductive gold nanoparticles on
403 PDDA–CNC/CGE has a detection limit of 2.4 μM , a sensitivity of 62.8 $\mu\text{A mM}^{-1} \text{cm}^{-2}$ for a linear
404 concentration range from 0.004 mM to 6.5 mM. B. Batra et al.^[69] developed an electrochemical
405 amperometric sensor based on chitosan supported by carboxylated multiwalled carbon nanotube
406 (cMWCNTs) and Au NPs on a gold electrode to detect glutamate. The strong electrostatic
407 interactions of chitosan and cMWCNTs boosted the sensitivity and selectivity of a sensor by

408 increasing the surface of the electrode and electron transfer (Figure 7). Satyanarayana et al.^[70] used
 409 Au NPs, multiwall carbon nanotubes (MWCNTs), and chitosan composites to identify 5-
 410 fluorouracil. The superstructure morphology has excellent electrocatalytic behavior and a large
 411 surface area. L. Ding et al.^[71] found that chitosan can be tuned into a bio-gel through a simple and
 412 green preparation method. They created an Au NPs/Chitosan nanocomposite gel for
 413 immobilization of K562 leukemia cells, with a limit of detection of 8.71×10^2 cells mL^{-1} at 10σ .
 414 Jodar et al.^[72] fabricated a conductive film filling with reduced graphene oxide, Au NPs, and potato
 415 starch to identify estriol. Starch from potato has excellent film-forming characteristics and is
 416 chemically stable. Cyclic voltammetry (CV) reading showed that the conducting film has a high
 417 peak current of 0.64 V and a detection limit of $0.48 \mu\text{mol L}^{-1}$, for a concentration range of 1.5 to
 418 $22 \mu\text{mol L}^{-1}$. Devasenathipathy et al.^[73] reported the use of CCLP as a stabilizer with Au NPs on
 419 MWCNTs to detect cysteine in food. The sensor exhibited a sensitivity of $0.46 \mu\text{A } \mu\text{M}^{-1}\text{cm}^{-2}$ and
 420 a detection limit of 19 nM, with a linear range from 0.1 to 1,000 μM . A picomolar determination
 421 of amitrole based on CCLP stabilized Au NPs showed a detection limit of 36 pM in a concentration
 422 range of 100 pM to 1500 pM through square wave voltammetry (SWV) analysis^[59].
 423



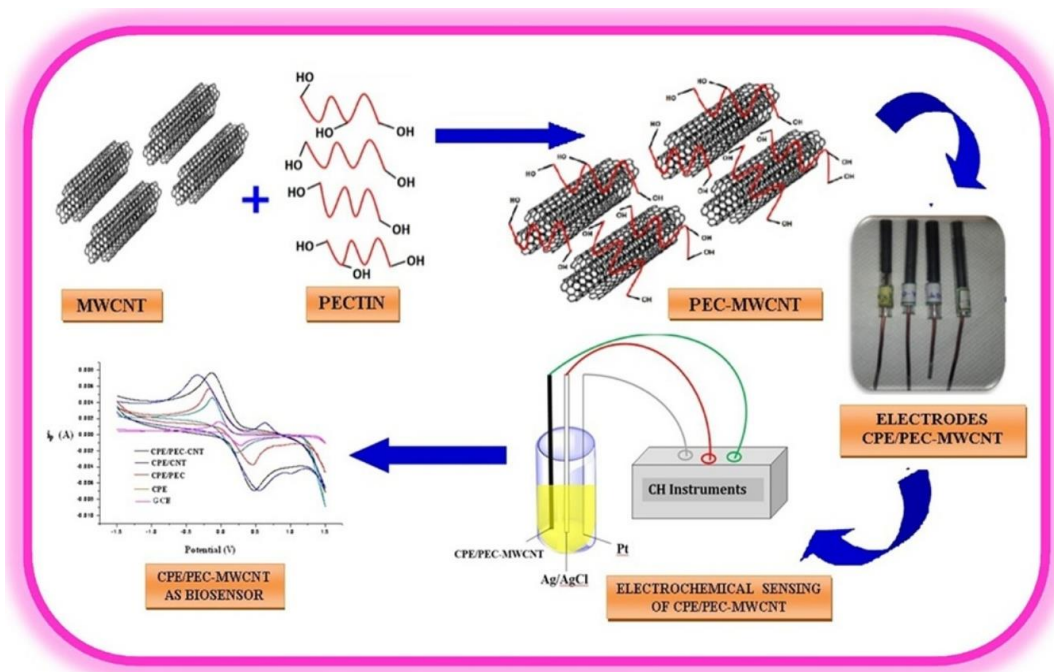
424

425 **Figure 7:** Schematic representation of chemical reaction involved in the fabrication of
 426 GluOx/cMWCNT/AuNP/CHIT/Au electrode. Reused with permission from Ref.^[69]. Copyright
 427 2013, Elsevier

428 *3.3 Biopolymer-carbon nanoparticles (CNPs)*

429 Shahrokhian et al.^[74] investigated the electro-analytical and uniform structure of CNFs and
430 CNPs on GCE to detect anticonvulsant agents. CNFs have a large porous surface with an adhesive
431 layer that prevents the CNPs from falling out of the surface. CNFs and CNPs have excellent
432 specific interconnectivity and compact adherence bonding, with long-term stability of the sensing
433 electrode surface, forming a linear response for clonazepam concentrations ranging from 0.1-10
434 μM and a detection limit of 0.08 μM . Carbon dots are distinctive nanoparticles, as it forms amine
435 and carboxyl groups in their structure when the carbon dots are dissolved in citric acid, resulting
436 in high permeability and good physiochemical properties. Sarkar et al.^[75] fabricated carbon dots-
437 based chitosan film as a sensing platform through microwave pyrolysis for a more reliable,
438 conductive, thermally stable with high mechanical firmness biosensor, to detect vitamin D in food.
439 Metallic and semiconducting nanoparticles were introduced on chitosan film to enhance the
440 selectivity, sensitivity, and electrical conductivity of an electrochemical glucose sensor^[76].
441 Positively charged chitosan was found to react with negatively charged composite metallic and
442 semiconducting materials, forming a stable platform for immobilization of glucose oxidase, which
443 prevents biomolecules from falling out and remaining in their folded state. Pectin extracted from
444 musk melon peels was used to alter MWCNT through the solvent casting method to create a non-
445 enzymatic sensing device to identify the creatinine biomarker, as shown in Figure 8. The pectin-
446 MWCNT matrix has excellent electron transfer tendency, large surface area, high diffusion
447 coefficient, good rate of electron transfer constant, and quick respond time. The matrix could
448 identify creatinine biomarker under normal conditions without the presence of enzymes.

449



450

451 **Figure 8:** Schematic representation of preparation of CPE/PEC-MWCNT and its efficiency in
 452 electrochemical sensing of creatinine. Reused with permission from Ref. [76]. Copyright 2018,
 453 Elsevier

454

455 3.4 Biopolymer-copper nanoparticles (Cu NPs)

456 Duran et al.^[77] carried out thermal decomposition pyrolysis on CNFs, forming carbonized
 457 CNFs, to increase carbon element content by integration of Cu NPs on CNFs. The carbonized
 458 CNFs/CuNPs have more micropores, larger surface area, good electrical conductivity, and good
 459 mechanical stability. The synthesized CNFs/Cu NPs/paper-based carbon electrode detects glucose
 460 by glucose oxidase (probe), with a sensitivity of $460 \pm 8 \mu\text{A cm}^{-2} \text{mM}^{-1}$ at linear response up to 3
 461 mM. Wang et al.^[78] developed a glucose and hydrogen peroxide dual function sensor on a matrix
 462 of chitosan modified covalently with copper (Cu) nanoparticles and carbon nanotube (CNT) on
 463 GCE. The presence of CNT on GCE can contribute significantly to the promotion of the
 464 electrochemical activity of the sensing electrode. This composite has a glucose detection limit of
 465 0.02 mM for concentrations ranging from 0.05 to 12 mM. Recently, a simple sonochemical method
 466 was used to fabricate copper ferrite nanoparticles (CuFe₂O₄ NPs)/chitosan composites. The large
 467 surface area and anti-fouling matrix of copper ferrite nanoparticles make it a suitable candidate to
 468 be doped on chitosan, to determine the 8-hydroxyguanine marker. This composite does not require
 469 a reducing or stabilizing agent, as chitosan is inherently stable. The copper ferrite nanoparticles

470 (CuFe₂O₄ NPs)/chitosan composite on a glassy carbon electrode electrochemical biosensor has a
471 concentration limit of 8.6 nM and a broad linear range from 0.025 to 697 μM ^[79]. As for lignin, the
472 coupling of lignin with copper oxide nanoparticles and the large surface area morphology of
473 MWCNTs improves the electrocatalytic activity and sensitivity of biosensors. Lignin serves as a
474 platform for identifying chlorogenic acid with numerous active sites due to the functional groups
475 present in lignin, which makes up the tubular nanocomposite strong π - π non-covalent bond,
476 resulting in an efficient interaction between probe and chlorogenic acid. This significantly boosts
477 the stability, as well as reproducibility, of the biosensor^[80]. The amorphous lignin can be shaped
478 and sized into nanoparticles with excellent rheological and physiochemical properties. The π - π
479 bond in lignin nanoparticles enhances the electron and charge transfer and further strengthens the
480 monooxygenase activity^[81]. The combination of Cu NPs with pectin and graphene through
481 electrodeposition to form graphene/pectin- Cu NPs were used for the detection of glucose and
482 hydrogen peroxide. Pectin was used as a scaffold with graphene as hybrid material support. The
483 Cu NPs conjugated pectin possesses stable, uniform, and physiochemical active properties, with a
484 relative standard deviation of 2.54 % for repeatability and 2.92 % for reproducibility. Graphene
485 facilitated the electrical conductivity of the hybrid material, with a sensitivity of 0.0457 μA
486 $\mu\text{M}^{-1}\text{cm}^{-2}$ and 0.391 μA $\mu\text{M}^{-1}\text{cm}^{-2}$ for the detection of glucose and hydrogen peroxide^[82].

487 3.5 Biopolymer-dual nanoparticles

488 Ranjbar et al.^[83] combined chemically synthesized Au NPs and CNPs on CNFs, forming a
489 biosensor for the detection of *Staphylococcus aureus*. Au NPs were utilized to facilitate the binding
490 of the thiolated aptamer (probe) on functionalized CNFs for porosity and electron transfer. E.
491 Darvishi et al.^[84] synthesized non-toxic and environmentally friendly nanoparticles using the
492 *Calendula officinalis L* plant to produce Au NPs and Ag NPs. The green Au NPs and Ag NPs
493 embedded on a cellulose quince seed mucilage platform were used to detect a biomarker for
494 prostate cancer. They proved that a green biosensor was possible to develop, with a detection limit
495 as low as 0.078 pg mL^{-1} with a biomarker concentration range from 0.1 pg mL^{-1} to 100 ng mL^{-1} .

496 3.6 Biopolymer-oxides nanoparticles

497 Jagadish et al.^[85] combined zinc oxide nanoparticles with starch through a wet chemical
498 method to detect caffeine. Starch controls the shape and size of zinc oxide by preventing the growth
499 and accumulation of nanoparticles. The zinc ion attaches to the hydroxyl group of starch in a warm
500 solution, as the crystalline structure of starch breaks down in a warm solution. The zinc oxide

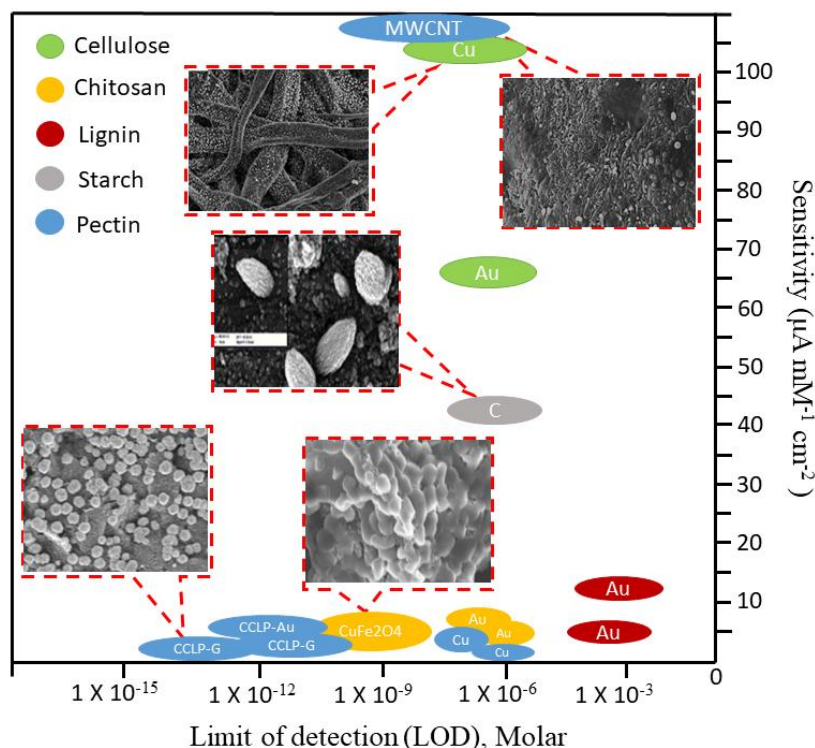
501 nanoparticles-based glassy carbon electrode showed a detection limit of 0.038 μM for a
502 concentration linear range of 2 to 100 μM . Using co-precipitation, starch was combined with
503 magnetic iron oxide nanoparticles to form a biosensor to detect folic acid (FA) using differential
504 pulse stripping voltammetry (DPSV), with a detection limit of 2.8 and 48 nM ^[86]. Cassava starch
505 has the potential as a basic functional polymer for biosensors. The combination of cassava starch
506 with a conductive material such as iron (II, III) oxide forming nanoparticles doped on molecularly
507 imprinted polymer (MIP) has been used to detect acetaminophen and caffeine. Cassava starch can
508 be cross-linked with conductive foreign material in a sodium hydroxide solvent, forming a polymer
509 material with basic functionality. These composite materials have a sensitivity of 0.5306 A/M for
510 the detection of acetaminophen and 0.4314 A/M for the detection of caffeine, with a detection limit
511 of 16 μM (acetaminophen) and 23 μM (caffeine)^[87]. Copper oxide nanoparticles enhance the
512 electrochemical oxidation of glycerol through amperometric measurement. The copper oxide
513 nanoparticles on MWCNT and pectin composite were used to detect glycerol in biodiesel, as pectin
514 can attract copper ions in a solution. Pectin facilitates the dispersion of the MWCNT
515 homogenously to produce repeatable results without the use of toxic chemicals such as dioxolane,
516 dimethylformamide, and dimethyl sulfoxide^[88].

517

518 *3.7 Biopolymer nanoparticles*

519 Biopolymers can be reshaped and resized into nanoparticles. Tortolini et al.^[89] developed
520 kraft lignin (sulfur filled) and organosolv lignin (sulfur free) nanoparticles for electrochemical eco-
521 friendly biosensing on a gold electrode. Chemical pulping and bioethanol production are two types
522 of processes that are used to extract sulfur lignin and sulfur-free lignin. The bonding between kraft
523 lignin nanoparticles with concanavalin A and glucose oxidase on gold electrode showed excellent
524 electrochemical probe and target interaction compared to organosolv lignin nanoparticles
525 composite. The kraft lignin nanoparticles and organosolv lignin nanoparticles showed a sensitivity
526 of (13.74 ± 1.84) and (4.53 ± 0.467) $\mu\text{AmM}^{-1} \text{cm}^2$ respectively, which led to stable sensing
527 devices, demonstrating that while lignin can augment the sensitivity of a biosensor, the analytical
528 performances depend on the number of lignin composites layers on the gold electrode. The
529 addition of nanoparticles in starch forming starch-nanoparticles composite significantly improves
530 crystallization kinetics, the morphology of the hybrid structure, crystal formation, crystalline size,
531 and overall mechanical and physical features of starch-nanoparticles composite^[90]. Starch is

532 extensively used as an alternative anchoring and stabilizing material in the formation of metal
 533 nanoparticles. The abundant network of glycoside bonds in starch acts as a stabilizer in a mixture
 534 solution to provide a surface passivation layer or protection, to avoid the accumulation of
 535 nanoparticles^[67]. Furthermore, starch can be used as an alternative carbon nanomaterial for the
 536 development of a sensing device. Das et al.^[91] used peeled potatoes as an alternative carbon source
 537 using pyrolysis and slow heating to obtain almond-shaped CNPs to detect sucrose. The unique
 538 properties of amylose and amylopectin in potatoes form conductive CNPs easily. The potato-based
 539 device is disposable and exhibits a sensitivity of $\sim 41.73725 \pm 0.01 \mu\text{AM}^{-1}\text{cm}^{-2}$, with a detection
 540 limit of $1 \mu\text{mol/L}$ through differential pulse voltammetry (DPV) and linear sweep voltammetry
 541 (LSV). The hydrothermal method at high temperature without a catalyst is another method to
 542 convert potato starch into a uniform and single carbon microsphere to detect Hg (II) ions^[92]. Figure
 543 9 shows the comparison of different biopolymer-based nanoparticle composites in an
 544 electrochemical sensor in terms of sensitivity and limit of detection (LOD). Table 1 summarizes
 545 biopolymers with nanoparticle composites electrochemical sensors.



546

547 **Figure 9:** Comparison of different biopolymer-based nanoparticles. High-performance by
 548 sensitivity and limit of detection (LOD) in electrochemical sensor. Inserted images are
 549 reproduced with permission from Ref. ^{[76][77][79][82][91]}. Copyright 2018, 2016, 2020, 2015, Elsevier

Bio polymer	Structure	Source	Electrode	Probe	Analyte	Technique	Linear Range	Limit of detection	Sensitivity	Real Sample	Ref
Cellulose	Nanocrystals		Ag/CNC/GCE	DNA	dsDNA	DPASV	1.0×10^{-11} - 1.0×10^{-7} mol L ⁻¹	2.3×10^{-11} mol L ⁻¹			[64]
	Nanofiber		CNFs/CNPs/GCE		clonazepam	LSV CV	0.1 – 10 μM	0.08 μM		Human serum	[74]
	Fibers		Cu NPs/cellulose fiber	Glucose oxidase	Glucose	CV	0 - 3 mM	5 μM	460 ± 8 μA cm ⁻² mM ⁻¹	Beverages	[77]
	Nanocrystals	Wood Pulp	Au/PDDA–CNC	Glucose oxidase	Glucose	CV	0.004 mM - 6.5 mM	2.4 μM	62.8 μA mM ⁻¹ cm ⁻²		[68]
	Nanofiber		Au NPs/Cu NPs/CNF	Aptamer	Staphylococcus aureus	CV EIS	1.2×10^1 - 1.2×10^8 CFU mL ⁻¹	1 CFU mL ⁻¹		Blood	[83]
	Quince seed mucilage	Quince seed mucilage	Quince seed mucilage/G NPs/SNPs	Antibody	Prostatic specific antigen (PSA)	EIS	0.1 pg mL ⁻¹ - 100 ng mL ⁻¹	0.078 pg mL ⁻¹		Human serum	[84]
Chitosan	Matrix		Cu/CHIT/CNT/GCE	Glucose oxidase	Glucose	EIS	0.05 - 12 mM	0.02 mM			[78]
	Film		GluOx/cMWCNT/Au NP/CHIT/Au electrode	Glutamate oxidase	Glutamate	CV EIS	5 – 500 μM	1.6 μM	155 nA/μM/cm ²	Sera	[69]

	Gel	Au NPs/CHIT/GCE	K562 Leukemia Cells	Cells	CV EIS	$1.34 \times 10^4 - 1.34 \times 10^8$ cells mL ⁻¹	8.71×10^2 cells mL ⁻¹			[71]
	Film	Au NPs-CS/PB-CS/Au electrode	β -glucanase	β -glucan	CV	6.25–93.75 μ M	1.56 μ M	100 nA μ M ⁻¹ cm ²	Red wine, Beijing Erguotou, Mianzhudaqu, Hericium, Oatmeal	[63]
	Nano composite Matrix	GNP-MWCNT-CHIT/GCE Ch@Ag NPs/SPGE	Ch@Ag NPs (probe)	5-fluorouracil Azidothymidine	CV DPV CV	0.03–10 μ M 10 μ M to 533 μ M	20 nM 1 μ M		Urine	[70]
	Composite	BSA/Ab/C-D-CH/ITO	antibody (Ab-VD2) / bovine serum albumin (BSA)	vitamin D	CV EIS	1 – 50 ng/mL	1.35 ng/mL	0.02 μ A ng ⁻¹ mL		[75]
	Nano structure	CuFe ₂ O ₄ /chitosan/GCE		8-hydroxyguanine	CV DPV	0.025–697.6 μ M	8.60 nM	2.807 μ A $\cdot \mu$ M ⁻¹ \cdot cm ⁻²	Blood serum, Urine	[79]
Lignin	Nano structure	LGN-MWCNT-CuONPs-GCE		Chlorogenic acid	CV DPV	5 μ M – 50 μ M	0.0125 μ M		Coffee	[80]
	Nano particles	LNPs/CAT LIG/HRP-GO _x /GCE	horseradish peroxidase	Glucose	CV	4.0 μ M - 16 μ M	0.85 μ M			[81]

				dase and glucos e oxidase	Chrom ogenic						
	Nano partic les	Oil pal m	LSG-NF- AgNPs	DNA	Tuberc ulosis	EIS	1 fM - 1 nM	1 fM			[66]
	Nano partic les	kraf lign in, org ano solv lign in	Au/SAMC ys/OLNPs/ ConA/GOx and Au/KLNPs /ConA/GO x	Conca navali n A, Glucos e oxidase	Glucos e	CV EIS	0.33 – 2.5 mM, 0.15 – 2.5 mM	0.11 mM, 0.05 mM	(4.53 ± 0.467) and (13.74 ± 1.84) μA mM ⁻¹ cm ²		[89]
Star ch	Almo nd- shape nanop articl es	potato	CNA		Sucrose	CV DPV LSV	1-100 μM	1 μmol/L	~41.7372 5 ± 0.01 μA·M ⁻¹ ·c m ⁻²	Fruit juices (Jack fruit, Mang o, Pinea pple)	[91]
	Film	potato	rGO- GNPs- PS/GCE		Estriol hormon e	CV	1.5 - 22 μmol L ⁻¹	0.48 μmol L ⁻¹		Tap water, river water, synth etic urine	[72]
	Nano partic les		ZnO-GCE		Caffein e	CV DPV	2–100 μM	0.038 μM		Bever ages	[85]
	Nano partic les		γ-Fe ₂ O ₃ nanoparticl es/GCE		folic acid	DPSV	0.05 - 1μM and 1 - 80μM	2.8 nM and 48 nM		Phar mace utical tablet s	[86]
	Mem brane	(cas sav a	GCE- M221- Fe ₃ O ₄		acetami nophen and caffein	DPV	50–2000 μM and 50–900 μM	16 and 23 μM	0.5306 A/M and 0.4314 A/M	Head ache medic ine	[87]

Pectin	Cross linked		CCLP-Au NPs/MWCNT/GCE	L-Cysteine	CV	0.1 – 1,000 μM	19 nM	0.46 $\mu\text{A cm}^{-2}$	Human blood serum	[73]
	Cross linked	citrus peel	CCLP-GNPs/GCE	amitrole	SWV	100-1500 pM 100-1500 nM	36 pM 20 nM	0.075 $\mu\text{A cm}^{-2}$, 0.1 $\mu\text{A nM}^{-1}$ cm^{-2}	Tap water, River water	[59]
	Scaffold	citrus peel	Graphene/pectin-CuNPs	Glucose, Hydrogen Peroxide	CV	10–5.5 μM 1 μM – 1 mM	2.1 μM 0.35 μM	0.0457 $\mu\text{A cm}^{-2}$, 0.391 $\mu\text{A cm}^{-2}$	Human serum, Contact lens cleaning solution on biodiesel	[82]
	Nanostructure		CuONP/Pectin(MWCNT)/GCE	glycerol	CV	9 x 10 ⁻³ – 1 mg L ⁻¹	5.8 x 10 ⁻³ mg L ⁻¹			[88]
	Nanostructure	muskel on peels	PEC-MWCNT/CPE	Creatinine	CV DPV	16 nM – 3.3 μM	0.6 μM	3550 $\mu\text{A cm}^{-2}$	urine	[76]

552 Ag, silver, CNC, cellulose nanocrystals, GCE, glass carbon electrode, CNF, cellulose nanofiber, CNPs, carbon
553 nanoparticles, Au, gold, PDDA-CNC, poly(diallyldimethylammonium chloride)-cellulose nanocrystal, Au NP &
554 GNPs, gold nanoparticles, SNPs & Ag NPs, silver nanoparticles, CHIT, CS, CH & Ch, chitosan, CNT, carbon
555 nanotubes, GluOx, glucose oxidase, cMWCNT, carboxylated multiwall carbon nanotubes, PB, prussian blue, BSA,
556 bovine serum albumin, Ab, antibody, CD, carbon dots, ITO, indium tin oxide, GOx, graphene oxide, CuFe₂O₄, copper
557 ferrite nanoparticles, LGN, lignin nanocomposite, CuONPs, copper oxide nanoparticles, LNPs, lignin nanoparticles,
558 CATLIG, cationic lignin, HRP, horseradish peroxidase, LSG-NF, laser scribed graphene nanoflower, OLNPs,
559 organosolv nanoparticles, KLNPs, kraft lignin nanoparticles, CNA, carbon nano almond, PS, potato starch, ZnO, zinc
560 oxide, $\gamma\text{-Fe}_2\text{O}_3$, maghemite, CCLP, calcium cross-linked pectin, SPGE, screen printed graphite electrode
561

562.0 Biopolymer with conducting or synthetic composite materials on electrochemical sensors

563 Conducting polymers are a special class of organic materials with the ability of overlapping
564 polymer molecular orbitals caused by extended π -conjugation structures along the polymer
565 backbone. The presence of cationic salts in conducting polymers modifies the physiochemical
566

567 properties and reversible reaction, as it has an oxidized state and a reduced state. Conducting
568 polymers have good compatibility, excellent electrical conductivity, chemical, and optical
569 properties, which improve electron-transfer efficiency and processability, extensively boosting
570 their popularity for biosensing applications. Synthetic polymers, on the other hand, has high carbon
571 content, high biostability, and resistance to degradation due to stacking carbon-carbon backbone.
572 Therefore, the coupling of biopolymers and conducting or synthetic polymers is one of the most
573 promising techniques for the development of these sensors, due to their relative stability, low
574 ionization potential, large surface area, redox conductivity, and optical features. As such,
575 biopolymer-based conducting polymers have been widely used in biosensors, due to their
576 significantly faster response time, having suitable features for interactions of biological elements
577 and morphology metrics, resulting in immediate charge and discharge reactions. Biosensors that
578 utilized biopolymer-based conducting or synthetic polymer are reviewed next.

579 *4.1 Biopolymer-polyaniline (PANI) composites*

580 PANI is one of the most studied conducting polymers, especially its potential electrical
581 properties and doping chemistry. It functions as an organic semiconductor with a semi-flexible
582 polymer. PANI is made up of aniline molecules through an oxidation acidic chemical reaction.
583 Several studies were conducted on PANI incorporating biopolymers, as PANI has weak
584 mechanical properties, weak ability to dissolve and inability to disperse uniformly in organic
585 solvents. The coupling of PANI and biopolymer through π - π bond forms intracellular matrices
586 with high volume surface area for the interaction of probe and target, to improve the capturing and
587 determination of a target. In-situ chemical polymerization, bottom-up and top-bottom applications
588 have been used to synthesize green-PANI/ multiwalled carbon nanotubes/ carboxymethyl cellulose
589 (PANI/MWCNTs/CMC) composites. The numerous hydroxyl and carboxyl groups found in CMC
590 allow protonated PANI to bind ionically with negatively charged CMC. Furthermore, the addition
591 of MWCNT rich with benzenoid rings increases the conductivity of the composite material. These
592 composite materials have a wide surface area per volume ratio, small pore diameter, and excellent
593 dissolution in organic solvents. The PANI/MWCNTs/CMC/CPE electrochemical biosensor has a
594 detection limit of ascorbic acid at 0.01 mM in 0.05mM⁻⁵ mM direct range and high sensitivity of
595 100.63 $\mu\text{AmM}^{-1} \text{ cm}^{-2}$, making PANI/MWCNTs/CMC composite materials suitable for the
596 detection of clinical biomarkers^[93]. Chitosan is also bonded with PANI, as chitosan has good
597 mechanical strength, excellent film-forming capability, and relatively good hydrophobicity. The

598 polycations of chitosan attract polyanions of other materials. A biopolymer bilayer using
599 protonated chitosan bonded with negatively charged carboxymethylpullulan, doped on PANI was
600 used as a transducer for the detection of urea^[94]. The electrostatic force between the amine group
601 of chitosan and carboxyl group of carboxymethylpullulan forms a mechanically excellent
602 biopolymer with PANI, increasing electrical conductivity. Kushwaha et al.^[95] added zinc oxide on
603 PANI-grafted chitosan composite to detect urea with enhanced sensitivity, as zinc oxide increased
604 the specific surface area and enhanced electron transfer. The sensitivity of the self-activating
605 tertiary hybrid material urea biosensor was $187.5 \mu\text{V ppm}^{-1} \text{cm}^{-2}$, with a detection limit of 29.84
606 ppm in the 20 ppm to 500 ppm range.

607 Gautam et al.^[48] interconjugated biopolymer starch with conducting polymer PANI doped
608 with carbon-filled MWCNTs forming PANI/MWCNTs/Starch nanocomposite. This
609 nanocomposite exhibits remarkable electrical conductivity, as the functional groups found in these
610 nanocomposites can disperse in organic and inorganic solvents easily with excellent
611 biocompatibility properties. This PANI/MWCNTs/Starch nanocomposite was used to determine
612 the presence of cholesterol in cow's milk. The covalently bonded starch with PANI and MWCNT
613 improves binding sites, electrocatalytic performances, and transfer of electrons, which led to the
614 oxidation of cholesterol. The nanocomposite has a high surface area and porous morphology that
615 enhances the hybridization of bioreceptors on the PANI/MWCNTs/Starch platform. This
616 cholesterol biosensor has a sensitivity of $800 \mu\text{A mM}^{-1} \text{cm}^{-2}$, with a detection limit of 0.01 mM in
617 the 0.032 to 5 mM range^[96]. The addition of hemoglobin on the PANI/MWCNTs/Starch
618 nanocomposite enables the detection of hydrogen peroxide and glucose by boosting the electrons'
619 charge transfer in terms of sensitivity and selectivity. The PANI/MWCNTs/Starch/HB
620 nanocomposite biosensor is stable, with a sensitivity of $76.43 \mu\text{A/mM cm}^2$ and a detection limit
621 of 0.032 Mm ^[97]. Thakur et al.^[57] used pectin on the surface of PANI to determine glucose in an
622 amperometric biosensor. The pectin biopolymer was dispersed homogenously in hydrochloric acid
623 and aniline mixture solution to avoid clumping. The pectin/ PANI composite has high water
624 dispersibility, excellent covalent bonding with glucose oxidase, porous morphological structure
625 (due to the gelatinous structure of pectin coated around PANI), and good electrical conductivity,
626 with pectin acting as a stabilizer and reducing agent. The efficiency of electron transfer during
627 amperometric analysis improved, leading to a sensitivity of $79.49 \mu\text{A mM}^{-1} \text{cm}^{-2}$ and a detection

628 limit of 43.5 μM . The pectin- PANI composite has a sensitivity three times better than conventional
629 PANI for glucose oxidase.

630 *4.2 Biopolymer-polypyrrole (PPy) composites*

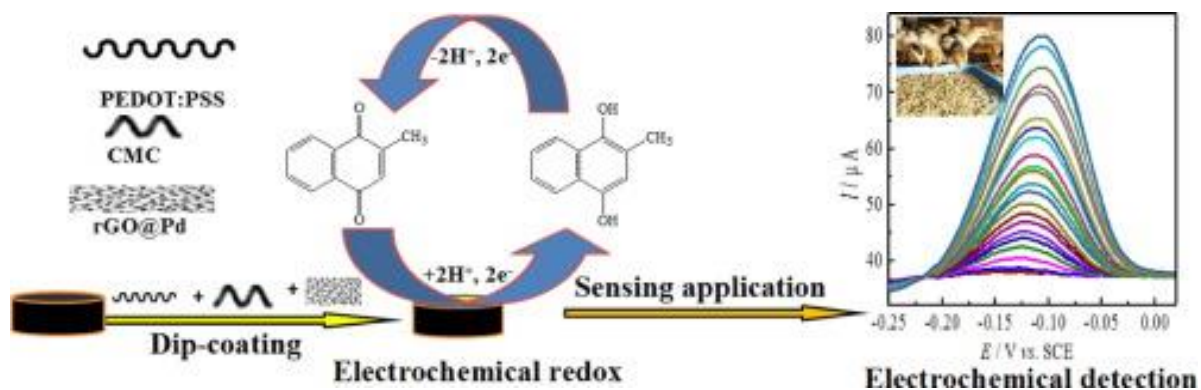
631 PPy is another type of conducting polymer that has a different polymer structure from
632 PANI with simpler polymerization and substitution, good physiochemical properties, controllable
633 polymer thickness, and excellent electrical conductivity. PPy is an organic polymer produced
634 through oxidative polymerization of pyrrole with formula $\text{H}(\text{C}_4\text{H}_2\text{NH})_n\text{H}$. A study conducted by
635 Esmaeili et al.^[26] found that the conjugation of polypyrrole-cellulose nanocrystal (PPy-CNC)
636 increased the performance of the biosensor in detecting glucose using glucose oxidase bioreceptor
637 such as PPy-CNC composite's unique physicochemical properties. The novel native structure of
638 PPy-CNC/SPE composite has a sensitivity of $0.73 \mu\text{A} \cdot \text{mM}^{-1}$ and a detection limit of (50 ± 10)
639 μM , with concentrations ranging from 1.0 to 20 mM. PPy-CNC/SPE sensors exhibit excellent
640 stability, retaining a DD of 95 % after 17 days and a relative standard deviation (RSD) of 4.47%
641 for repeatability. Recently, Uzunçar et al.^[98] developed a biocompatible electrochemical biosensor
642 for common interfering compounds on indium tin oxide coated glass electrodes. They synthesized
643 PPy, carboxymethylcellulose (CMC) together with Prussian Blue nanoparticles (PBNPs)
644 peroxidase to overcome the dispersibility limitation of PPy in solution and to enhance the electrical
645 conduction of the PPy polymer chain. The CMC stabilizes the composite material and enhances
646 the affinity for solutions such as water. The CMC-PPy-PBNPs/ITO sensor platform can detect
647 hydrogen peroxide and glucose as well. The glucose sensing platform has a sensitivity of 456.8
648 $\mu\text{A} \text{mM}^{-1} \text{cm}^{-2}$ and a detection limit of $5.23 \mu\text{M}$ within a range of 20 to $1100 \mu\text{M}$, while the
649 hydrogen peroxide sensor platform had a sensitivity of $456.8 \mu\text{A} \text{mM}^{-1} \text{cm}^{-2}$ and a detection limit
650 of $0.59 \mu\text{M}$ in a rectilinear range of 5 and $470 \mu\text{M}$. PPy nanotubes and gold nanoparticles
651 strengthen the electrical conductivity, although the nanocomposite has poor reproducibility. The
652 high structural mechanical strength of PPy conducting polymer and gold nanoparticles resisted the
653 breaking of the bond, allowing for better reusability. Chitosan in PPy nanotubes and gold
654 nanoparticles nanocomposite has excellent biocompatibility and eases the breaking of bonds,
655 enabling the biosensor to regenerate by reverse surface modification reaction^[38]. Chitosan-PPy-
656 gold nanoparticles nanocomposite has better charge transportation efficiency and provides a proper
657 platform for enzyme connectivity for the detection of xanthine, with a $0.25 \mu\text{M}$ detection limit in
658 the 1 to $200 \mu\text{M}$ ^[99] range.

659 Bulk PPy has slow electron transfer, which affects the sensitivity of a sensing surface. The
660 addition of chitosan and metal oxide to conducting polymer forms a stable, conductive, large
661 surface area, biocompatible, simple, reproducible, and selective composite film, which acts as an
662 active material for biosensor development. The amphipathic nature of chitosan and PPy makes it
663 a suitable coupled material for opto-chemical sensing. The PPy-chitosan-iron oxide nanoparticles
664 on indium tin oxide (ITO) glass displayed an amperometric response with a limit of glucose
665 identification of 234 μM in the 1 to 16 mM range^[100]. Starch is a polysaccharide that can be used
666 as a template or morphology-directing agent to form a one-dimensional conducting polymer. The
667 formation of a one-dimensional conducting polymer is very challenging in terms of biomolecule
668 degradation and optimization of biopolymer amino-acid growth. Uniform-sized PPy nanowires
669 were synthesized by dissolving pyrrole in soluble starch, with the pyrrole monomers attracting
670 starch molecules via hydrogen attachment formed between pyrrole and the hydroxyl group of
671 starch^[47]. Polymerization occurs along the chain of starch, which forms the PPy nanowires. The
672 linear chain of amino acids in starch combines with functional groups as a template. The coupling
673 of starch with conducting polymers has many applications, especially in electrochemical sensing.
674 The combination of the contrasting properties of starch and conducting polymer has excellent
675 synergic effects and allows simpler modification. Generally, almost all conducting polymers such
676 as PPy and PANI possess bonding capabilities and electron charge transfer ability when foreign
677 material is present. The combination of starch with a conducting polymer causes an electron
678 exchange or the attraction of opposite ions, which changes the conductivity, physiochemical, and
679 optical properties of the hybrid material. As pectin and PPy have similar nitrogen and oxygen
680 atoms, they exhibit good mechanical strength and ease in forming amides in an aqueous ammonia
681 mixture to form films. Arulraj et al.^[101] added graphene in pectin/PPy composite as supporting
682 material, to enhance conductivity and to provide a larger surface area to absorb mercury ions. The
683 graphene/PPy/pectin composite has a detection limit of mercury ions as low as femtomolar, with
684 a sensitivity of 28.64 $\mu\text{A } \mu\text{M}^{-1}$. Biopolymers such as pectin are rich in galacturonic acid and can
685 act as a biopolymer electrolyte in biosensors, forming proton-conducting biopolymer electrolytes
686 embedded with ammonium chloride and ammonium bromide. Notably, pectin-ammonium
687 bromide electrolyte film has excellent optimized ionic conductivity and good electrical properties
688 compared to pectin-ammonium chloride. This is because pectin-ammonium bromide has poor
689 lattice energy and larger anionic size, as well as high dielectric constant and dielectric loss^[102].

690 4.3 Biopolymer-poly(3,4-ethylenedioxythiophene) (PEDOT) composites

691 Poly(3,4-ethylenedioxythiophene) (PEDOT) and poly(styrene sulfonate) (PSS) are two of the
692 most important noble carbon conducting polymers that are chemically stable, environmentally
693 friendly, conductive, have fewer network defects with the capability to dope as well as reverse its
694 doping properties. A conductive, synergistic electrochemical sensor with excellent electron
695 transfer was developed by integrating (PEDOT:PSS) composite conducting polymer with
696 carboxymethyl cellulose (CMC) and reduced graphene oxide@palladium (rGO@Pd) for the
697 detection of vitamin K₃ (VK₃) using voltammetric analysis, as shown in Figure 10^[103]. CMC can
698 overcome the limitations of PEDOT:PSS in terms of substrate interface, brittle structure defects,
699 and weak fixative force between PEDOT and PSS. It is capable of enhancing and strengthening
700 the carbon structure of PEDOT:PSS composites and provides a stable and long-lasting sensing
701 GCE. The synergistic composite electrode has a 1.4×10^{-8} M detection limit for a 4×10^{-7} to $9 \times$
702 10^{-5} M concentration range.

703



704

705 **Figure 10:** The fabrication procedure of PEDOT:PSS-CMC-rGO@Pd/GCE for the voltammetric
706 determination of vitamin K₃ in real samples. Reproduced with permission from Ref. ^[103].

707

Copyright 2016, Elsevier

708

709 Xu et al. developed carboxylated cellulose nanocrystals (CNCC) through chemical treatment
710 on microcrystalline cellulose and ammonium persulfate doped with Ag NPs on CNCC. The
711 PEDOT conducting polymer was integrated with Ag NPs/CNCC substrate with excellent catalytic
712 activity in detecting dopamine through an oxidation process. The PEDOT/ Ag NPs/CNCC/GCE
713 electrochemical sensor detected dopamine at a low detection limit of 17 nM in the range of 0.05
714 to 782 μ M, and retained a 93.2% stability after 1 month with an RSD value of 5.8 % for

715 repeatability and 3.97 % for reproducibility^[104]. They also modified PEDOT/Fe₃O₄-CNCC with
716 GCE using a similar oxidation-reduction method to produce CNCC from microcrystalline
717 cellulose to detect nitrite in food. The addition of Fe₃O₄ increased the transfer of charged electrons
718 of the composite transducer with a 0.1 μM detection limit for a nitrite concentration range of 0.5
719 – 2500 μM. The PEDOT/Fe₃O₄-CNCC/GCE sensor has an excellent synergistic effect with a 4.7
720 % loss in stability in 2 weeks and a relative standard deviation (RSD) of 4.6 % for repeatability
721 and 3.7 % for reproducibility^[105].

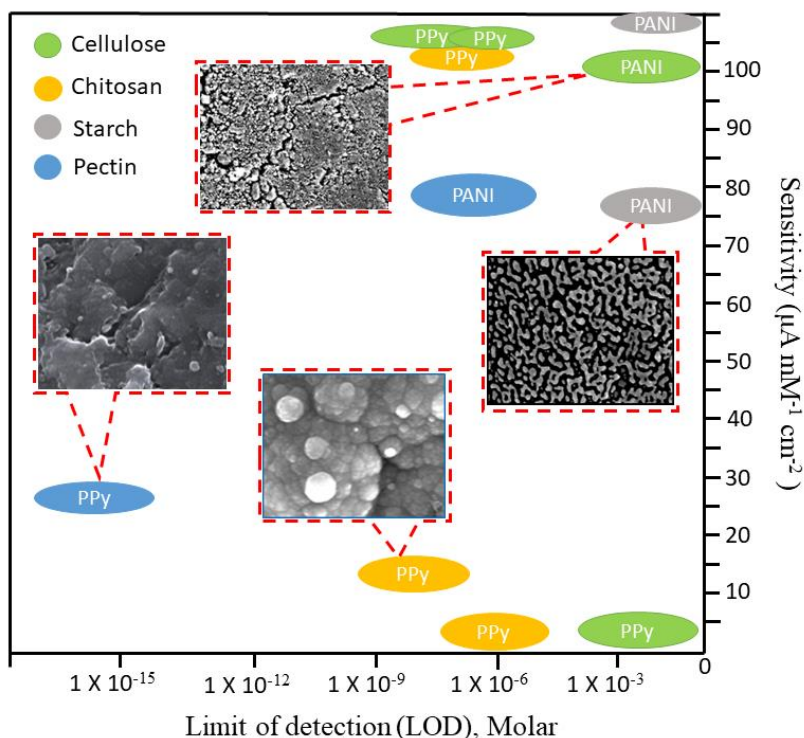
722 *4.4 Biopolymer-polyacrylonitrile (PAN) composites*

723 PAN is a type of synthetic semicrystalline resin from the polymerization of acrylonitrile.
724 It has a linear formula of (C₃H₃N) and has been extensively used as a precursor in the
725 electrospinning technique for use in biosensors because it is a petroleum-based polymer that has
726 high resistance to chemicals and good membrane formation. However, the electrospinning heating
727 process of PAN is time-consuming and requires high operating costs. To overcome these
728 drawbacks, biorefinery lignin is used as a replacement for PAN, as lignin has a 68 % carbon
729 content and can be electrospun easily^[106]. Mustafov et al.^[107] blended lignin and PAN, forming
730 carbon-filled nanofibers through an electrospinning technique doped with conductive graphene to
731 develop a highly activated platform on a screen-printed electrode to detect acetaminophen. The
732 diameter of the composite nanofibers depends on the mass of lignin and the temperature of the
733 carbonization process. They concluded that the large surface area of lignin/PAN/graphene is one
734 of the factors that enhances the sensitivity of acetaminophen biosensors. It should be noted that
735 the detection of a biopolymer and synthetic polymer electrochemical biosensor is related to
736 detectable changes in the electrical properties of these materials, which is proportional to the
737 concentration of a specific biological element. Apart from PAN, molecularly imprinted conducting
738 polymers are used for the detection of condensed lignin molecules in pulping industries. Lignin
739 can combine with a synthetic polymer to form functional groups^[108].

740 *4.5 Biopolymer-polyurethanes composites*

741 Poor solubility in organic solvents affecting the dissolution of lignin in a polymer matrix
742 is one of the biggest challenges to forming lignin-polymer composites. Lignin's structure is easily
743 modified as lignin contains oligometric and low-weight polymeric particles that can be separated
744 into a liquidized mixture. The covalent binding of lignin (hydroxyl group) with polymer
745 (isocyanate group) can be formed through condensation, as lignin has an OH group that forms

746 polyurethanes^[43]. While polyurethanes have good stability, they are not conductive. The
747 combination of lignin-polymer with a conductive material using percolation is therefore necessary,
748 especially when used as a conducting polymer. Kraft lignin polyurethane doped with MWCNT
749 has excellent ion transfer properties, which makes it an excellent sensing platform candidate^[109].
750 Gonçalves et al.^[110] used polyurethane-kraft lignin with carbon nanotube composites as a
751 potentiometric sensor to detect copper (II) ions, demonstrating that polyphenolic groups found in
752 that composite material enhance the selectivity and sensitivity. A. Rudnitskaya et al.^[111] formed
753 polyurethanes by co-polymerization with tolylene 2,4-diisocyanate terminating poly(propylene
754 glycol) using various types of lignin namely, kraft lignin, lignosulphate, and organosolv lignin to
755 form polyurethanes embedded with MWCNT. The lignin-based polyurethanes/carbon nanotubes
756 composites are highly conductive active material candidates for chromium (VI) determination,
757 with a detection limit of 5.0×10^{-6} M within the range of 1×10^{-5} M to 1×10^{-2} M. Carbon
758 nanotube boosts the electrical conductivity of substrate used as sensing platform on glass sensor
759 whereas organosolv lignin and lignosulphate have a very sensitive sensing surface, especially in
760 an acid mixture. The strong C-C structural bonding between carbon filled carbon nanotubes with
761 numerous type functional groups of lignin make the sensor stable, rigid, and reproducible.
762 Lignocellulose has more than two hydroxyl groups and can be passed down as polyols for organic
763 polyurethane preparation. Lignocellulose has the tendency to escalate the electrochemical
764 reactions by interacting with metal sulfides. Figure 11 shows the sensitivity and LOD of various
765 biopolymer based conducting polymer and synthetic polymers composites electrochemical sensor.
766 Table 2 shows electrochemical sensors based on biopolymers with conducting polymers
767 composites.



768

769 **Figure 11:** Comparison of different biopolymer-based polymers (conducting or synthetic) by
 770 sensitivity and limit of detection (LOD) in electrochemical sensor. Inserted images are
 771 reproduced with permission from Ref. ^{[93][97][100][101]}. Copyright 2018,2016, Elsevier

772

773 **Table 2:** Literature on biopolymers-based polymers (conducting or synthetic) composites in
 774 electrochemical sensor

Biopolymer	Structure	Source	Electrode	Probe	Analyte	Technique	Linear Range	Limit of detection	Sensitivity	Real Sample	Ref
Cellulose	Hydrogel		PANI/MWCNTs/CMC		Ascorbic acid	CV	0.05 mM – 5 mM	0.01 mM	100.63 $\mu\text{A} \cdot \text{mM}^{-1} \text{cm}^{-2}$		[93]
	Nanocrystal		SPE/PPy/CNC/GluOx	Glucose oxidase	Glucose	DPV	1.0 to 20 mM	0.05 mM	0.73 $\mu\text{A} \cdot \text{mM}^{-1}$	Glucose solution	[26]
	Nanostructure		ITO/CMC-PPy-PB		Glucose, Hydrogen peroxide	CV	20 – 1100 μM , 5 – 470 μM	5.23 μM , 0.59 μM	456.8 $\mu\text{A} \cdot \text{mM}^{-1}$	Milk, Tap water	[98]

	Nanost ructure		PEDOT:PSS- CMC- rGO@Pd/GC E	Vita min K3	LSV EIS CV	4×10^{-7} to 9×10^{-5} M	1.4×10^{-8} M		Animal blood and feedstuf f	[103]
	Nanoc rystal		PEDOT/AgN Ps/CNCC/GC E	Dopa mine	CV EIS	0.05 - 782 μ M	17 nM		Human urine	[104]
	Nanoc rystal		PEDOT/Fe3O 4-CNCC/GCE	Nitrit e	DPV CV	0.5– 2500 μ M	0.1 μ M		Pickles	[105]
Chit osan	Nanost ructure		Urs/ZnO- en/CHIT-g- PANI/ITO	Urea	Potenti ometric	20 ppm - 500 ppm (0.3 mM - 8.3 mM)	29.84 ppm	187.5 μ V ppm^{-1} cm^{-2}	Human blood serum	[95]
	Nanot ubes		Chi/PPy- NTs/Au- NPs/ITO	Glucos e oxidase	Glucos e EIS CV	3–230 μ M	3.10 μ M	149 μ A μM^{-1} mL		[38]
	Film		Chitosan/PPy/ AuNPs/GCE	Xanth ine	CV EIS	1 – 200 μ M	0.25 μ M	1.4 nA/ μ M	Meat	[99]
	Film		PPy-CS- Fe ₃ O ₄ NP/ITO	Glucos e	Amper ometric	1 – 16 mM	234 μ M	12 μ A cm^{-2} mM^{-1}		[100]
Lign in	Memb rane	Kraf t pulpi ng of euca lypt woo d (Euc alypt us glob ulus)	Kraft lignin/MWCN Ts	Copp er (II) ions	Potenti ometric					[110]
	Nanofi ber		Lignin/PAN/ GRP/SPE	Aceta mino phen	EIS DPV					[107]
	Kraft lignin,	kraft pulpi ng of	lignin-based polyurethanes /MWCNTs	Cr(VI)	Potenti ometric	1×10^{-5} M	5.0×10^{-6} M	20 mV pX^{-1} (Kraft)		[111]

	Organosolv lignin	euca lyptus wood (E. globulus), spruce wood (P. abies)				$-1 \times 10^{-2} \text{ M}$		and 21 mV pX ⁻¹ (Organosolv)		
Starch	Nanost ructure	PANI/MWCN Ts/Starch/CP E	Glucose oxidase	Cholesterol	CV EIS	0.032 to 5 mM	0.01 mM	800 $\mu\text{A cm}^{-2} \text{ mM}^{-1}$	Cow milk	[96]
	Nanost ructure	PANI/MWCN Ts/Starch/HB/CPE, PANI/MWCN Ts/Starch/HB/GluOx/CPE	Glucose oxidase	Hydrogen peroxide and glucose	CV EIS	0.1 mM – 5 mM	0.032 mM	76.43 $\mu\text{A cm}^{-2} \text{ mM}^{-1}$		[97]
Pectin	Nanop articles	GluOx-PANI-Pect NPs/Pt	Glucose oxidase	Glucose	CV	0.06 – 4 mM	43.5 μM	79.49 $\mu\text{A cm}^{-2} \text{ mM}^{-1}$	Human blood serum	[57]
	Film	PPy/Pct/GR/G CE		Mercuric ions	DPAS V	2 μM - 29 μM	4 fM	28.64 $\mu\text{A cm}^{-2} \text{ mM}^{-1}$	Tap water	[101]

775 PANI, polyaniline, SPE, screen printed electrode, CMC, carboxymethyl cellulose, PPy, polypyrrole, PEDOT,
776 poly(3,4-ethylenedioxy thiophene), PSS, poly(styrene) sulfonate, Pd, palladium, CNCC, carboxylated cellulose
777 nanocrystals, Fe₃O₄, iron (II,III) oxide, Urs, urease, CNC, cellulose nanocrystals, GCE, glass carbon electrode, Au
778 NP, gold nanoparticles, Ag NPs, silver nanoparticles, CHIT, CS, & Chi, chitosan, GluOx, glucose oxidase, MWCNTs,
779 multiwall carbon nanotubes, PB, prussian blue, ITO, indium tin oxide, rGO, reduced graphene oxide, ZnO, zinc oxide,
780 CPE, carbon paste electrode, HB, hemoglobin, NTs, nanotubes, PAN, polyacrylonitrile, GRP & GR, graphene, Pec
781 NPs, pectin nanoparticles, Pct, pectin, Pt, platinum.
782

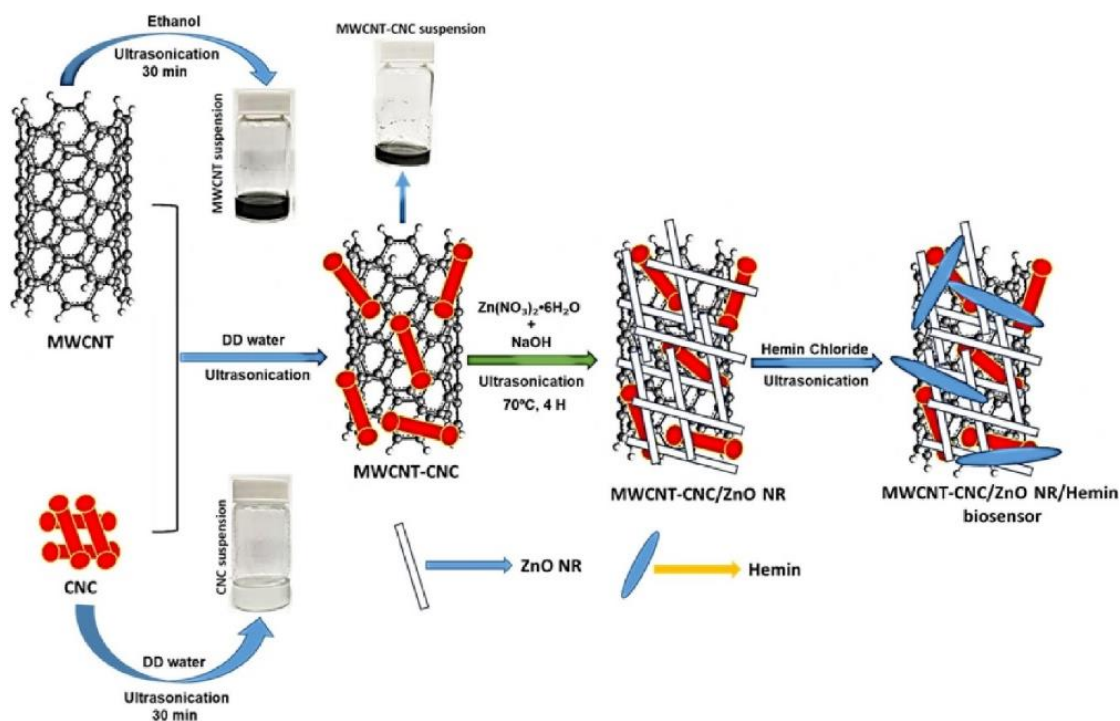
785.0 Biopolymer with nanomaterial composite on electrochemical sensor

784 Biopolymers based on nanomaterials including metal oxides, graphene, molybdenum
785 disulfide, and nanodiamonds are promising candidates for use in electrochemical biosensors.
786 These nanomaterials have remarkable features namely, comparable sizes with biological
787 molecules and unique mechanical, electrical, thermal, and multifunctional properties. Any analyte

788 interaction on the biopolymer-nanomaterials will result in a significant change in the electrical
789 properties as well.

790 5.1 Biopolymer-metal oxides

791 There are abundant metal oxides, but only certain oxides have been widely used in
792 electrochemical biosensors such as zinc, iron, manganese, and copper. The conductivity and
793 crystalline morphology structure of metal oxides induce electron mobility on a stable surface with
794 easy bonding biopolymer. Metal oxides are synthesized mainly through the hydrothermal and sol-
795 gel methods. Covalent bonding of metal oxides with biopolymer helps to overcome its
796 hydrophobic drawback. Palanisamy et al.^[112] developed cellulose nanocrystals biopolymer and
797 hexagonal nanorods of ZnO conjugation deposited on MWCNT through sonochemical and
798 ultrasonication for ultrasensitive electrochemical detection of hydrogen peroxide (H_2O_2), as shown
799 in Figure 12. The substrate platform interacts to form iron protoporphyrin instead of an enzyme,
800 for better analytical reaction through cyclic voltammetry. The detection limit of this novel
801 substrate on screen-printed carbon electrode (SPCE) is 4.0 nM at concentrations up to 4183.3 μM .
802



803

804 **Figure 12:** Pictorial depiction for the solution based sonochemical synthesis of ZnO and
805 MWCNT-CNC/ZnO NR composite and fabrication of the MWCNT-CNC/ZnO NR/hemin
806 biosensor. Reused with permission from Ref. ^[112]. Copyright 2020, Elsevier

807 Iron oxide/nanocellulose crystalline composite deposited on a screen-printed carbon electrode
808 was used to detect *Mycobacterium tuberculosis* (TB)^[113]. This iron oxide/nanocellulose composite
809 has low discernment at 7.96×10^{-13} M for concentrations in the 1.0×10^{-6} to 1.0×10^{-12} M range.
810 Khalilzadeh et al.^[114] developed a magnetic iron oxide@cellulose nanocrystals with copper using
811 a plant extract (*Petasites hybridus* leaf) as a stabilizing and reducing agent for copper to detect
812 venlafaxine. The sensor has a detection limit of 0.01 μ M for venlafaxine with concentrations range
813 between 0.05 to 600 μ M. Chen et al.^[40] developed a layer-by-layer deposition of manganese oxide
814 in the form of nanoflakes with chitosan, with these materials interacting strongly due to opposite
815 charges formed in them. Manganese oxide and chitosan improve physical and chemical properties,
816 which enhances the oxidation of hydrogen peroxide with a sensitivity of $0.038 \text{ A M}^{-1} \text{ cm}^{-2}$, as
817 chitosan is used as a polyelectrolyte consisting of positively charged ions that facilitates layer-by-
818 layer modification. Electrostatic interaction when combining chitosan with nickel ferrite and
819 copper oxide is significant in biosensing applications. Chitosan has remarkable biocompatibility
820 and the ability to form films, with nickel ferrite having excellent stability in catalytic chemical
821 interactions to bond with chitosan. Copper oxide can enhance the electron transfer efficiency, as it
822 is a monoxide medium. These nanocomposite substances result in high sensitivity of
823 $0.043 \mu\text{A}/(\text{mg/L cm}^{-2})$, with a detection limit of 313 mg/L^[115]. Yazhini et al.^[116] developed a hetro-
824 metal oxides nanohybrid composite on pectin as a scaffold that has efficient shuttling of electrons
825 for sensing applications, as the nanohybrids acquire synergistic effect due to the attachment of
826 hetro-metal oxides nanohybrid to the pectin by $-\text{OH}$ binding. The blending of copper oxide and
827 iron oxide was made through co-precipitation method and ultrasonication, grown on a pectin
828 matrix extracted from musk melon peels. The hetro-metal oxides nanohybrid composited has good
829 electrocatalytic reactions as copper oxide and iron oxide are biocompatible, have easily modifiable
830 structure, and have a highly charged surface. Liu et al.^[117] developed pectin-derived carbon with
831 cobalt (II, III) oxide to form a hollow nanosphere surface morphology that overcomes the major
832 problems of cobalt (II, III) oxide in terms of high temperature and low response, with pectin acting
833 as a soft template. The hollow nanostructure improves the transportation of electrons which
834 directly effects the analytical performance in detecting hydrogen peroxide. Pectin derived carbon
835 with cobalt (II, III) oxide biosensor has a sensitivity of $405.8 \mu\text{A}\cdot\text{mM}\cdot\text{cm}^{-2}$ and a detection limit
836 of 0.30 μ M.

837 5.2 Biopolymer-graphene

838 Graphene is a single layer of carbon atoms, strongly bound in a hexagonal honeycomb lattice.
839 It has an allotrope of carbon in the form of a plane of sp^2 bonded atoms with a molecular bond
840 length of 0.142 nm. Its derivatives such as reduced graphene, graphene oxide, and nitrogen-doped
841 graphene oxide have the best electrical conductivity of any material. Even though graphene is a
842 non-metal, it has a good specific surface area, extraordinary electronic properties, fast electron
843 transport abilities, and ultra-flexibility. It is an excellent conductor with biopolymer owing to its
844 large surface area and good film assembly, making the combination of graphene and especially
845 chitosan an important substrate. A layer-by-layer method fabrication of a glucose biological
846 sensor^[118] resulted in the accumulation of biorecognition such as glucose oxidase on chitosan, by
847 conjugating nitrogen embedded graphene on chitosan with a sensitivity of $10.5 \mu\text{A cm}^{-2} \text{mM}^{-1}$
848 and a detection limit of 64 μM . Adumitrăchioaie et al.^[119] developed an electrochemical sensor
849 based on chitosan and graphene oxide for the detection of serotonin. Graphene's carboxylic group
850 interacts with antibodies covalently, while chitosan stabilized the nanocomposite deposited on an
851 electrode during the sensing of serotonin concentrations, with a detection limit of 3.2 nM in the
852 range of 10 nM to 100 μM . Similarly, the covalently bonded nanocomposite of graphene and
853 chitosan structure can be modified into film and nanoribbons by blending for glucose, guanine,
854 adenine, thymine, and cytosine determination^[120, 121]. Krishna. R et al.^[122] synthesized reduced
855 graphene oxide/nickel nanoparticles (rGo-Ni NPs) deposited onto glassy carbon electrode as a
856 hybrid nanocomposite film of chitosan and glucose oxidase. The developed glucose sensor showed
857 a sensitivity up to $129 \mu\text{A cm}^{-2} \text{Mm}^{-1}$ at a low operating potential.
858 Starch is also capable of forming a film, as it has two carbohydrate units that have different
859 structures and roles, amylose and amylopectin. Amylose forms a film when it attaches to water,
860 forming hydrogen bonds with water and further reducing water affinity to form a matrix. Orzari et
861 al.^[123] developed a highly conductive film using manioc starch and reduced graphene oxide for
862 phenolic compound detection. The functional groups in Manioc starch form π - π bonds with
863 reduced graphene oxide to enhance the functionality of the film and electrical conductivity.
864 Graphene disperses easily in polymers, which increases the surface area and the interactive sensing
865 surface. This film sensor can detect dopamine and catechol with a detection limit of 0.07 and 0.04
866 $\mu\text{mol L}^{-1}$, respectively through CV analysis. Starch can also be extracted from seeds such as
867 *Artocarpus heterophyllus* to create a nitrogen bonded porous carbon material with high magnetic

868 strength, indestructible carbon-nitrogen bond, a large surface area, and porous surface
869 morphology, which facilitates the transfer of electrons sensing interface. The nitrogen bonded
870 porous carbon material exhibits excellent electrochemical stability, reproducibility, sensitivity
871 ($4.64 \mu\text{A } \mu\text{M}^{-1} \text{cm}^{-2}$), and a low detection limit (2.74 nM) in detecting dopamine. The interactions
872 of starch-based nitrogen bonded porous carbon materials with dopamine were stronger at -0.64 eV
873 compared to oxygen-filled sheets^[124]. Apart from metal oxides, graphene oxide has been widely
874 used as a conductive substrate. However, the charged ions diffusion in graphene is limited due to
875 the non-reversible aggregation or accumulation of hydrophobic sheets attached by van der Waals
876 interaction in graphene. The conjugation of graphene oxides with pectin in an electrochemical
877 sensor is necessary due to the presence of functional groups, with graphene oxide interfacial
878 adhesion of pectin. Graphene oxide sheets exhibits good functionality, with smaller substrates
879 forming a large surface area, enhancing the electrons transportation with low resistance ions
880 compared to bulk graphene. Pectin and reduced graphene oxide was coupled to form a
881 nanocomposite to detect dopamine and paracetamol, with a detection limit of 1.5 and 1.8 nM
882 respectively through linear sweep voltammetry (LSV) techniques^[125].

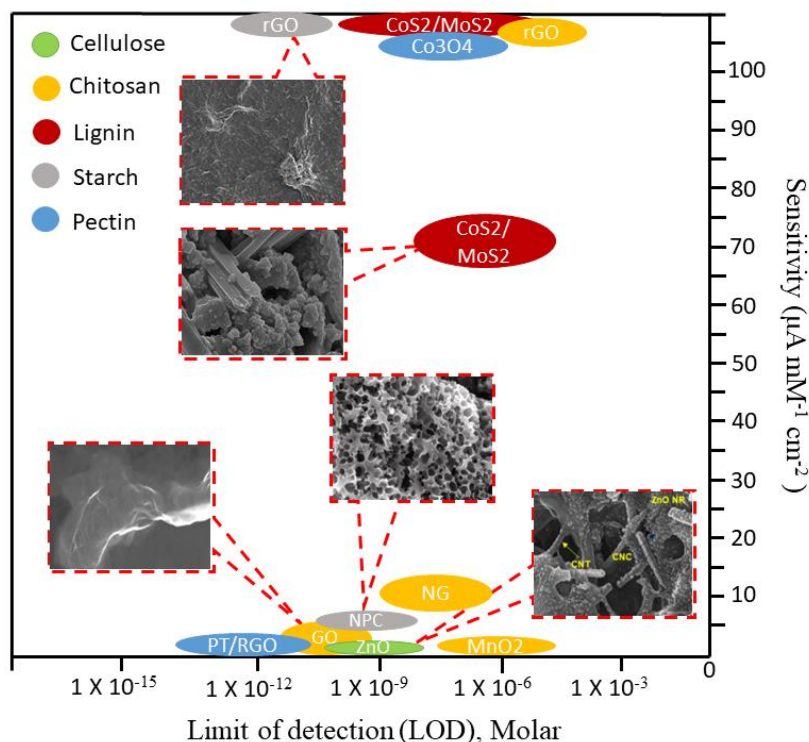
883 *5.3 Biopolymer-molybdenum disulfide (MoS₂)*

884 Wang et al.^[126] used molybdenum disulfide (MoS₂) for electrical conductivity in a
885 cellulose-based substrate, as cellulose has poor conductivity. MoS₂ is derived from a transition
886 metal, where molybdenum is placed in group 6, whereas chalcogen is from group 16 in the periodic
887 table. MoS₂ layered semiconductor with a band gap of 1.2 eV can resist oxidation at temperatures
888 of up to 85°C. Cellulose from a straw can be modified structurally to a carbon nanotube structure
889 using TEMPO-mediated oxidation. The TEMPO-oxidized straw cellulose underwent the
890 hydrothermal method with a MoS₂ precursor to allow MoS₂ to grow at the edges of the TEMPO-
891 oxidised straw cellulose (TOSC) surface. The TOSC substrate was subsequently used to detect
892 nitrite. The composite substrate has an efficient signal transfer as cellulose nanofiber has a larger
893 surface area and semi-crystallinity, whereas MoS₂ is a semi-conducting metal with graphene-like
894 structure. This combination of materials enhances the detection of nitrite, with a detection limit of
895 $2.0 \mu\text{M}$ in wide linear ranges of 6.0–3140 and 3140–4200 μM . Zhang et al.^[127] found that cobalt
896 disulfide (CoS₂) and MoS₂ incorporated with nitrogen-doped lignocellulose improved the
897 efficiency of electron transportation during ascorbic acid, dopamine, and nitrite identification on

898 glass carbon electrode with a sensitivity of $4941.8 \mu\text{A } \mu\text{M}^{-1}$ for ascorbic acid, $73.3 \mu\text{A } \mu\text{M}^{-1}$ for
899 dopamine and $5732.9 \mu\text{A } \mu\text{M}^{-1}$ for nitrite.

900 *5.4 Biopolymer-nanodiamonds*

901 Starch is an alternative biopolymer for carbon synthesis. Starch from potatoes and tapioca
902 has unique properties to convert into carbon, especially when a high thermal process is applied,
903 with an increased solubility. The concentration of starch in a metal mixture solution determines
904 the electrochemical performance of a sensor. Starch, in particular potato starch, has good chemical
905 stability, is easy to modify, inexpensive, can be found abundantly in nature, and is biocompatible.
906 Camargo et al.^[128] developed a toxic-free potato starch coupled with nanodiamonds for catechol
907 detection. The conductive synergistic matrix forms a remarkably large surface area that eases the
908 deposition of tyrosinase (enzyme) to detect catechol with a detection limit of $3.9 \times 10^{-7} \text{ mol L}^{-1}$
909 with a linear range from 5.0×10^{-6} to $7.4 \times 10^{-4} \text{ mol L}^{-1}$ through differential pulse voltammetry
910 (DPV) measurements. N.A. Zambianco et al.^[129] developed nanodiamond nanoparticles
911 conjugated with manioc starch to detect herbicide diquat (DQ) in environmental samples. The
912 composite material is structurally stable, and has good analytical performance with efficient
913 electron transfer, with a detection limit of $1.1 \times 10^{-7} \text{ mol L}^{-1}$ from a linear range of 5.0×10^{-7} to
914 $4.6 \times 10^{-5} \text{ mol L}^{-1}$. Fernandes-Junior et al.^[130] found that nanodiamonds improved electrochemical
915 surface area and strengthen the manioc starch film polymeric mechanical nanocomposite structure
916 for the detection of tetracycline. Figure 13 shows various biopolymer-based metal composites
917 electrochemical sensors of their sensitivity and LOD. Table 3 summarises biopolymers with metal
918 composite electrochemical sensors.



919

920 **Figure 13:** Comparison of different biopolymer- based nanomaterials composites by sensitivity
 921 and limit of detection (LOD) in electrochemical sensor. Reproduced with permission from
 922 Ref.^{[112][119][123][124][127]}. Copyright 2020,2019,2018,2021,2017, Elsevier

923

924 **Table 3:** Literature on biopolymer-based nanomaterials composites in electrochemical sensor

Biopolym er	Struct ure	Source	Electrode	Prob e	Anal yte	Tech nique	Linear Range	Limit of detection	Sensiti vity	Real sample	Ref
Cellulose	Nanofiber	Straw pulp	TOSC-MoS ₂ /GCE		Nitrite	CV	6 – 3140 μM, 3140 – 4200 μM	2.0 μM		Drinking water, River water	[126]
	Nanocrystals	Cotton linters	MWCNT-CNC/ZnO NR/He/SPCE		Hydrogen Peroxide	CV	0.01 – 4183.3 μM	0.004 μM	0.134 μA μM ⁻¹	Milk (low-fat)	[112]
	Nanocrystals	Plant extract (Petasites hybridus leaf)	Fe ₃ O ₄ @CNC/Cu/G SPE		Venlafaxine	CV DPV	0.05 – 600.0 μM	0.01 μM		Urine, Water, Pharmaceutical formulation	[114]

					(DA), Nitrite		0.5 – 5160 μM		$\mu\text{M}^{-1}\text{cm}^{-2}$, 5732.9 $\mu\text{A}\mu\text{M}^{-1}\text{cm}^{-2}$			
Starch	Nanost ructure	Potato	Tyr-ND-PS/GCE	Tyros inase	Catec hol	DPV CV	5.0×10^{-6} – 7.4×10^{-4} mol L^{-1}	3.9×10^{-7} mol L^{-1}			Tap water, River water	[128]
	Nanost ructure	Manioc	ND-MS/GCE		Diqua t	SWV	5.0×10^{-7} to 4.6×10^{-5} mol L^{-1}	1.1×10^{-7} mol L^{-1}			River water, Drinkin g water	[129]
	Film	Manioc	ND-MS/GCE		Tetra cyclin e	DPV	5 – 180 $\mu\text{mol L}^{-1}$	2.0 $\mu\text{mol L}^{-1}$			Water, Wells water	[130]
	Film	Manioc (Manih ot species)	rGO-MS/GCE		Dopa mine, Catec hol	CV	0.5 – 200 $\mu\text{mol L}^{-1}$, 0.5 – 74 $\mu\text{mol L}^{-1}$	0.07 $\mu\text{mol L}^{-1}$, 0.04 $\mu\text{mol L}^{-1}$	2913 $\mu\text{A}(\mu\text{mol L}^{-1})^{-1}\text{cm}^{-2}$		Water, Syntheti c urine	[123]
	Nanost ructure	Artocar pus heterop hyllus seeds	NPC/GCE		Dopa mine	EIS CV DPV	30 – 90 μM , 200 – 400 μM	2.74 nM	4.64 $\mu\text{A}\mu\text{M}^{-1}\text{cm}^{-2}$		Human serum, Urine	[124]
Pecti n	Hydro gel		PT/rGO/G CE		Dopa mine, Parac etamo l	CV LSV	0.003 – 90.206 μM , 0.003– 91.04 μM	1.5 nM, 1.8 nM	5.71 $\mu\text{A}\mu\text{M}^{-1}\text{cm}^{-2}$, 3.896 $\mu\text{A}\mu\text{M}^{-1}\text{cm}^{-2}$		human serum, Pharmac eutical	[125]
	Nanop article s		hs-S300-Co3O4/C-GCE		Hydr ogen Perox ide	Ampe romet ric	0.90 μM – 5.98 mM	0.30 μM	405.8 $\mu\text{A}\cdot\text{mM}\cdot\text{cm}^{-2}$		Tap water, River water	[117]

925 SPE, screen printed electrode, CNC, cellulose nanocrystals, GCE, glass carbon electrode, GluOx, glucose oxidase,
926 MWCNTs, multiwall carbon nanotubes, rGO, reduced graphene oxide, ZnO NR, zinc oxide nanoribbon, TOSC,
927 TEMPO-oxidised straw cellulose, MoS₂, molybdenum disulfide, He, hemin, Cu, copper, MPA, mercaptopropionic
928 acid, CTAB, cetyl trimethyl ammonium bromide, PEI, polyethylenimine, rGO, reduced graphene oxide, Ni, nickel,
929 MnO₂, manganese (IV) oxide, NG, nitrogen doped graphene, ITO, indium tin oxide, PSS, poly(styrene sulfonate),
930 AuQC, gold quartz crystal, ChOx, cholesterol oxidase, NiFe₂O₄, nickel ferrite, CuO, copper oxide, FeO, iron oxide,
931 CH, chitosan, GONRs, graphene oxide nanoribbons, N-LC, nitrogen doped lignocellulose, CoS₂, cobalt sulfide, Tyr,
932 tyrosinase, ND, nanodiamond, PS, potato starch, MS, manioc starch, NPC, nitrogen porous carbon, PT, pectin, Co₃O₄,
933 cobalt (II,III) oxide.
934

935.0 Conclusions and future perspectives

936 Significant progress has been made in recent years on biopolymers for electrochemical
937 sensors, especially on the structural composition of cellulose, chitosan, lignin, starch, and pectin
938 conjugated with nanoparticles, polymers, and nanomaterials. Biopolymers are mainly for
939 biochemical modification in electrochemical sensors, enhancing their bio-functionality, electron
940 transfer, conductivity, and biochemical reaction. In summary, cellulose, with its large and porous
941 structure, forms numerous active sites for bioreceptors to capture analytes (target), increasing its
942 sensitivity. Chitosan is the most promising substrate for enzyme immobilization due to its
943 biocompatibility and multiple functional groups. It has free amino acids in its structure, which
944 improves its solubility and active sites. It can be altered easily while retaining its original
945 properties, and it can interact with bioactive molecules such as antibodies and enzymes.
946 Meanwhile, lignin can be modified into functionalized lignin through simple chemical
947 modifications as a biosensor substrate. Alteration in its aliphatic and phenolic alcohol through
948 acetylation creates hydrocarbons that can be easily attached to any solvents and compounds.
949 Starch's biggest advantage is having a reducing agent. As such, no additive such as formic acid or
950 oxalic acid is needed in the fabrication of a hybrid material. Pectin, on the other hand, has a
951 stabilizer that traps covalently bonded enzymes and proteins. Conjugating biopolymers with
952 conductive nanomaterials like nanoparticles, conducting polymers and metal oxides forming
953 conductive composite substrates enhance the analytical performances of the biosensor. Pectin
954 biopolymer tends to give the best LOD for nanoparticles (CCLP/Au NPs)^[59], polymers
955 (Pectin/PPy)^[101] and nanomaterials (Pectin/rGO)^[125] composites biosensors. In all three
956 composites considered, pectin biopolymer has the lowest LOD (better than picomolar) compared
957 to other biopolymer composites. Unfortunately, pectin biopolymer composites do not have the best
958 surface sensitivity due to their hydrophobic characteristics, swelling under acidic condition, and

959 fragile surface. Composites that display the best LOD have borderline sensitivity reading. The
960 biosensor with the highest sensitivity to date is those with the combination of Pectin/MWCNT^[76],
961 Starch/PANI^[96], and Lignin/CoS₂/MoS₂^[127]. Pectin/rGO/GCE^[125] and
962 Lignin/CoS₂/MoS₂/GCE^[127] biosensors can detect multiple analytes, although there are huge
963 differences in LODs. Biopolymers increase the number of active sites, allowing more bioreceptors
964 to be captured on a composite material. Indeed, these biopolymers have proven their efficiency in
965 bonding through cross-linking, covalent, electrostatic and entrapment processes, with bioreceptor
966 to detect targets. Conductive additive materials have been used to enhance the conductivity of the
967 biopolymers, with biopolymers serving as a stabilizing, reducing, and absorbent agent for rapid
968 response. Additionally, the production cost is reduced when using biopolymers instead of
969 expensive engineered polymers. An ideal biosensor would be one that can detect multiple analytes
970 in the lowest analyte concentration, highest sensitivity and highest selectivity. Deciding the right
971 composite in a biosensor is challenging, with the choice depending on the analyte, sensitivity, and
972 selectivity required. Future work should look at the development of a multi-analyte biosensor that
973 is highly sensitive and selective, made from composites that are biodegradable and based on
974 environmentally friendly technology. Additionally, the performance of carrageenan, alginates and
975 pullulan composites should be compared with reviewed biopolymers for electrochemical
976 biosensors.

977 **References**

978

- 979 [1] Pohanka, M.; Skládal, P. Electrochemical Biosensors - Principles and Applications. *J.*
980 *Appl. Biomed.*, **2008**, 6 (2), 57–64. <https://doi.org/10.32725/jab.2008.008>.
- 981 [2] Torati, S. R.; Reddy, V.; Yoon, S. S.; Kim, C. G. Electrochemical Biosensor for
982 Mycobacterium Tuberculosis DNA Detection Based on Gold Nanotubes Array Electrode
983 Platform. *Biosens. Bioelectron.*, **2016**, Vol. 78, 483–488.
984 <https://doi.org/10.1016/j.bios.2015.11.098>.
- 985 [3] Yoon, H.; Nah, J.; Kim, H.; Ko, S.; Barman, S. C.; Xuan, X.; Kim, J.; Park, J. Y.
986 Chemically Modified Laser-Induced Porous Graphene Based Flexible and Ultrasensitive
987 Electrochemical Biosensor for Sweat Glucose Detection. *Sensors and Actuators B :*
988 *Chemical A*, **2020**, Vol. 311, p 127866. <https://doi.org/10.1016/j.snb.2020.127866>
- 989 [4] Goud, K. Y.; Reddy, K. K.; Satyanarayana, M.; Kummari, S.; Gobi, K. V. A Review on
990 Recent Developments in Optical and Electrochemical Aptamer-Based Assays for
991 Mycotoxins Using Advanced Nanomaterials. *Microchim. Acta*, **2020**, 187(1):29.
992 <https://doi.org/10.1007/s00604-019-4034-0>.

- 993 [5] Xue, Q. The Development and Application of Geosynthetics. *Appl. Mech. Mater.*, **2013**,
994 253–255 (PART 1), 489–492. <https://doi.org/10.4028/www.scientific.net/AMM.253->
995 255.489.
- 996 [6] Forouzanfar, S.; Alam, F.; Pala, N.; Wang, C. A Review of Electrochemical Aptasensors
997 for Label-Free Cancer Diagnosis. *J. Electrochem. Soc.*, **2020**, *167* (6), p 067511.
998 <https://doi.org/10.1149/1945-7111/ab7f20>.
- 999 [7] Zamay, G. S.; Zamay, T. N.; Kolovskii, V. A.; Shabanov, A. V.; Glazyrin, Y. E.;
1000 Veprintsev, D. V.; Krat, A. V.; Zamay, S. S.; Kolovskaya, O. S.; Gargaun, A.; et al.
1001 Electrochemical Aptasensor for Lung Cancer-Related Protein Detection in Crude Blood
1002 Plasma Samples. *Nat. Publ. Gr.*, **2016**, No. October, 1–8.
1003 <https://doi.org/10.1038/srep34350>.
- 1004 [8] Cesewski, E.; Johnson, B. N. Electrochemical Biosensors for Pathogen Detection.
1005 *Biosensors and Bioelectronics*. **2020**, Vol. *159*, p 112214.
1006 <https://doi.org/10.1016/j.bios.2020.112214>.
- 1007 [9] Habib, S.; Ghodsi, E.; Abdollahi, S.; Nadri, S. Porous Graphene Oxide Nanostructure as
1008 an Excellent Scaffold for Label-Free Electrochemical Biosensor : Detection of Cardiac
1009 Troponin I. **2016**, Vol. *69*, 447–452. DOI: 10.1016/j.msec.2016.07.005
- 1010 [10] Chang, I.; Jeon, M.; Cho, G. C. Application of Microbial Biopolymers as an Alternative
1011 Construction Binder for Earth Buildings in Underdeveloped Countries. *Int. J. Polym. Sci.*,
1012 **2015**, Vol. *2015*. p 326745. <https://doi.org/10.1155/2015/326745>.
- 1013 [11] Kumar, S.; Sarita; Nehra, M.; Dilbaghi, N.; Tankeshwar, K.; Kim, K. H. Recent Advances
1014 and Remaining Challenges for Polymeric Nanocomposites in Healthcare Applications.
1015 *Progress in Polymer Science*. **2018**, Vol. *80*, pp 1–38.
1016 <https://doi.org/10.1016/j.progpolymsci.2018.03.001>.
- 1017 [12] Selvaraj, T.; Perumal, V.; Khor, S. F.; Anthony, L. S.; Gopinath, S. C. B.; Muti Mohamed,
1018 N. The Recent Development of Polysaccharides Biomaterials and Their Performance for
1019 Supercapacitor Applications. *Materials Research Bulletin*. **2020**, Vol. *126*, p 110839.
1020 <https://doi.org/10.1016/j.materresbull.2020.110839>.
- 1021 [13] Lahcen, A. A.; Rauf, S.; Beduk, T.; Durmus, C.; Aljedaibi, A.; Timur, S.; Alshareef, H.
1022 N.; Amine, A.; Wolfbeis, O. S.; Salama, K. N. Electrochemical Sensors and Biosensors
1023 Using Laser-Derived Graphene: A Comprehensive Review. *Biosensors and*
1024 *Bioelectronics*. **2020**, Vol. *168*, p 112565. <https://doi.org/10.1016/j.bios.2020.112565>.
- 1025 [14] Kanmani, P.; Aravind, J.; Kamaraj, M.; Sureshbabu, P.; Karthikeyan, S. Environmental
1026 Applications of Chitosan and Cellulosic Biopolymers: A Comprehensive Outlook.
1027 *Bioresource Technology*. **2017**, pp 295–303.
1028 <https://doi.org/10.1016/j.biortech.2017.03.119>.
- 1029 [15] Jian, M.; Zhang, Y.; Liu, Z. Natural Biopolymers for Flexible Sensing and Energy
1030 Devices; **2020**; Vol. *38*. <https://doi.org/10.1007/s10118-020-2379-9>.
- 1031 [16] Hassan, M. E.; Bai, J.; Dou, D. Q. Biopolymers; Definition, Classification and
1032 Applications. *Egypt. J. Chem.*, **2019**, *62* (9), 1725–1737.

- 1033 <https://doi.org/10.21608/EJCHEM.2019.6967.1580>.
- 1034 [17] Kamel, S.; Khattab, T. A. Recent Advances in Cellulose-Based Biosensors for Medical
1035 Diagnosis. *Biosensors*, **2020**, *10*(6), 67. <https://doi.org/10.3390/BIOS10060067>.
- 1036 [18] Wang, Z.; Ma, Z.; Sun, J.; Yan, Y.; Bu, M.; Huo, Y.; Li, Y. F.; Hu, N. Recent Advances in
1037 Natural Functional Biopolymers and Their Applications of Electronic Skins and Flexible
1038 Strain Sensors. *Polymers (Basel)*, **2021**, *13* (5), 1–18.
1039 <https://doi.org/10.3390/polym13050813>.
- 1040 [19] Zargar, V.; Asghari, M.; Dashti, A. A Review on Chitin and Chitosan Polymers: Structure,
1041 Chemistry, Solubility, Derivatives, and Applications. *ChemBioEng Rev.*, **2015**, *2* (3), 204–
1042 226. <https://doi.org/10.1002/cben.201400025>.
- 1043 [20] Romero, M.; Macchione, M. A.; Mattea, F.; Strumia, M. The Role of Polymers in
1044 Analytical Medical Applications. A Review. *Microchemical Journal*. **2020**, Vol. *159*, p.
1045 105366. <https://doi.org/10.1016/j.microc.2020.105366>.
- 1046 [21] Zhao, D.; Zhu, Y.; Cheng, W.; Chen, W.; Wu, Y.; Yu, H. Cellulose-Based Flexible
1047 Functional Materials for Emerging Intelligent Electronics. *Adv. Mater.*, **2020**, *2000619*, 1–
1048 18. <https://doi.org/10.1002/adma.202000619>.
- 1049 [22] Swingler, S.; Gupta, A.; Gibson, H.; Kowalczyk, M.; Heaselgrave, W.; Radecka, I. Recent
1050 Advances and Applications of Bacterial Cellulose in Biomedicine. *Polymers (Basel)*,
1051 **2021**, *13* (3), 1–29. <https://doi.org/10.3390/polym13030412>.
- 1052 [23] Yue, X.; Feng, J.; Li, H.; Xiao, Z.; Qiu, Y.; Yu, X.; Xiang, J. Novel Synthesis of Carbon
1053 Nanofiber Aerogels from Coconut Matrix for the Electrochemical Detection of Glucose.
1054 *Diam. Relat. Mater.*, **2021**, *111* (October 2020), 108180.
1055 <https://doi.org/10.1016/j.diamond.2020.108180>.
- 1056 [24] Maduraiveeran, G. Bionanomaterial-Based Electrochemical Biosensing Platforms for
1057 Biomedical Applications. *Anal. Methods*, **2020**, *12* (13), 1688–1701.
1058 <https://doi.org/10.1039/d0ay00171f>.
- 1059 [25] Culica, M. E.; Chibac-Scutaru, A.-L.; Mohan, T.; Coseri, S. Cellulose-Based Biogenic
1060 Supports, Remarkably Friendly Biomaterials for Proteins and Biomolecules. *Biosensors
1061 and Bioelectronics*. **2021**, Vol. *182*, p 113170. <https://doi.org/10.1016/j.bios.2021.113170>.
- 1062 [26] Esmaeili, C.; Abdi, M. M.; Mathew, A. P.; Jonoobi, M.; Oksman, K.; Rezayi, M. Synergy
1063 Effect of Nanocrystalline Cellulose for the Biosensing Detection of Glucose. *Sensors
1064 (Switzerland)*, **2015**, *15* (10), 24681–24697. <https://doi.org/10.3390/s151024681>.
- 1065 [27] Das, S.; Ghosh, B.; Sarkar, K. Nanocellulose as Sustainable Biomaterials for Drug
1066 Delivery. *Sensors Int.*, **2022**, *3* (October 2021), 100135.
1067 <https://doi.org/10.1016/j.sintl.2021.100135>.
- 1068 [28] Terzopoulou, Z. N.; Papageorgiou, G. Z.; Papadopoulou, E.; Athanassiadou, E.;
1069 Alexopoulou, E.; Bikiaris, D. N. Green Composites Prepared from Aliphatic Polyesters
1070 and Bast Fibers. *Ind. Crops Prod.*, **2015**, *68*, 60–79.
1071 <https://doi.org/10.1016/j.indcrop.2014.08.034>.

- 1072 [29] Zhang, M.; Gorski, W. Electrochemical Sensing Platform Based on the Carbon
1073 Nanotubes/Redox Mediators-Biopolymer System. *J. Am. Chem. Soc.*, **2005**, *127* (7),
1074 2058–2059. <https://doi.org/10.1021/ja044764g>.
- 1075 [30] Wei, X.; Zhang, M.; Gorski, W. Coupling the Lactate Oxidase to Electrodes by Iontropic
1076 Gelation of Biopolymer. *Anal. Chem.*, **2003**, *75* (9), 2060–2064.
1077 <https://doi.org/10.1021/ac020765k>.
- 1078 [31] Zhang, M.; Smith, A.; Gorski, W. Carbon Nanotube-Chitosan System for Electrochemical
1079 Sensing Based on Dehydrogenase Enzymes. *Anal. Chem.*, **2004**, *76* (17), 5045–5050.
1080 <https://doi.org/10.1021/ac049519u>.
- 1081 [32] Darder, M.; López-Blanco, M.; Aranda, P.; Aznar, A. J.; Bravo, J.; Ruiz-Hitzky, E.
1082 Microfibrinous Chitosan - Sepiolite Nanocomposites. *Chem. Mater.*, **2006**, *18* (6), 1602–
1083 1610. <https://doi.org/10.1021/cm0523642>.
- 1084 [33] Yamada, M.; Honma, I. Anhydrous Proton Conductive Membrane Consisting of Chitosan.
1085 *Electrochim. Acta*, **2005**, *50* (14), 2837–2841.
1086 <https://doi.org/10.1016/j.electacta.2004.11.031>.
- 1087 [34] Darder, M.; Colilla, M.; Ruiz-Hitzky, E. Chitosan-Clay Nanocomposites: Application as
1088 Electrochemical Sensors. *Appl. Clay Sci.*, **2005**, *28* (1-4 SPEC. ISS.), 199–208.
1089 <https://doi.org/10.1016/j.clay.2004.02.009>.
- 1090 [35] Jiang, Y.; Wu, J. Recent Development in Chitosan Nanocomposites for Surface-Based
1091 Biosensor Applications. *Electrophoresis*, **2019**, *40* (16), 2084–2097.
1092 <https://doi.org/10.1002/elps.201900066>.
- 1093 [36] Suginta, W.; Khunkaewla, P.; Schulte, A. Electrochemical Biosensor Applications of
1094 Polysaccharides Chitin and Chitosan. *Chem. Rev.*, **2013**, *113* (7), 5458–5479.
1095 <https://doi.org/10.1021/cr300325r>.
- 1096 [37] Boyles, M. S. P.; Kristl, T.; Andosch, A.; Zimmermann, M.; Tran, N.; Casals, E.; Himly,
1097 M.; Puentes, V.; Huber, C. G.; Meindl, U. L.; et al. Chitosan Functionalisation of Gold
1098 Nanoparticles Encourages Particle Uptake and Induces Cytotoxicity and pro -
1099 Inflammatory Conditions in Phagocytic Cells , as Well as Enhancing Particle Interactions
1100 with Serum Components. *J. Nanobiotechnology*, **2015**, 1–20.
1101 <https://doi.org/10.1186/s12951-015-0146-9>.
- 1102 [38] Sharma, A.; Kumar, A. Study of Structural and Electro-Catalytic Behaviour of
1103 Amperometric Biosensor Based on Chitosan/Polypyrrole Nanotubes-Gold Nanoparticles
1104 Nanocomposites. *Synthetic Metals*. **2016**, Vol. 220, pp 551–559.
1105 <https://doi.org/10.1016/j.synthmet.2016.07.012>.
- 1106 [39] Mohammadi, B.; Pirsá, S.; Alizadeh, M. Preparing Chitosan – Polyaniline Nanocomposite
1107 Film and Examining Its Mechanical , Electrical , and Antimicrobial Properties. *Polym.*
1108 *Polym. Compos.*, **2019**, *27* (8), 507–517. <https://doi.org/10.1177/0967391119851439>.
- 1109 [40] Chen, X.; Zhang, X.; Yang, W.; Evans, D. G. Biopolymer-Manganese Oxide Nanoflake
1110 Nanocomposite Films Fabricated by Electrostatic Layer-by-Layer Assembly. *Mater. Sci.*
1111 *Eng. C*, **2009**, *29* (1), 284–287. <https://doi.org/10.1016/j.msec.2008.06.024>.

- 1112 [41] Juntapram, K.; Praphairaksit, N.; Siraleartmukul, K.; Muangsin, N. Synthesis and
1113 Characterization of Chitosan-Homocysteine Thiolactone as a Mucoadhesive Polymer.
1114 *Carbohydr. Polym.*, **2012**, *87* (4), 2399–2408.
1115 <https://doi.org/10.1016/j.carbpol.2011.11.007>.
- 1116 [42] Tang, L.; Zeng, G. M.; Wang, H.; Shen, G. L.; Huang, D. L. Amperometric Detection of
1117 Lignin-Degrading Peroxidase Activities from Phanerochaete Chrysosporium. *Enzyme*
1118 *Microb. Technol.*, **2005**, *36* (7), 960–966.
1119 <https://doi.org/10.1016/j.enzmictec.2005.02.009>.
- 1120 [43] Klapiszewski, Ł.; Wysokowski, M.; Majchrzak, I.; Szatkowski, T.; Nowacka, M.;
1121 Siwińska-Stefańska, K.; Szwarc-Rzepka, K.; Bartczak, P.; Ehrlich, H.; Jesionowski, T.
1122 Preparation and Characterization of Multifunctional Chitin/Lignin Materials. *J.*
1123 *Nanomater.*, **2013**, Vol. 2013. <https://doi.org/10.1155/2013/425726>.
- 1124 [44] Saratale, R. G.; Saratale, G. D.; Ghodake, G.; Cho, S. K.; Kadam, A.; Kumar, G.; Jeon, B.
1125 H.; Pant, D.; Bhatnagar, A.; Shin, H. S. Wheat Straw Extracted Lignin in Silver
1126 Nanoparticles Synthesis: Expanding Its Prophecy towards Antineoplastic Potency and
1127 Hydrogen Peroxide Sensing Ability. *International Journal of Biological Macromolecules*.
1128 **2019**, pp 391–400. <https://doi.org/10.1016/j.ijbiomac.2019.01.120>.
- 1129 [45] Degefu, H.; Amare, M.; Tessema, M.; Admassie, S. Lignin Modified Glassy Carbon
1130 Electrode for the Electrochemical Determination of Histamine in Human Urine and Wine
1131 Samples. *Electrochim. Acta*, **2014**, Vol. 121, 307–314.
1132 <https://doi.org/10.1016/j.electacta.2013.12.133>.
- 1133 [46] Zakzeski, J.; Bruijninx, P. C. A.; Jongerius, A. L.; Weckhuysen, B. M. The Catalytic
1134 Valorization of Lignin for the Production of Renewable Chemicals. *Chem. Rev.*, **2010**,
1135 *110* (6), 3552–3599. <https://doi.org/10.1021/cr900354u>.
- 1136 [47] Shi, W.; Liang, P.; Ge, D.; Wang, J.; Zhang, Q. Starch-Assisted Synthesis of Polypyrrole
1137 Nanowires by a Simple Electrochemical Approach. *Chem. Commun.*, **2007**, No. 23, 2414–
1138 2416. <https://doi.org/10.1039/b701592e>.
- 1139 [48] Gautam, V.; Srivastava, A.; Singh, K. P.; Yadav, V. L. Preparation and Characterization
1140 of Polyaniline, Multiwall Carbon Nanotubes, and Starch Bionanocomposite Material for
1141 Potential Bioanalytical Applications. *Polym. Polym. Compos.*, **2015**, *11* (2).
1142 <https://doi.org/10.1002/pc>.
- 1143 [49] Chivrac, F.; Pollet, E.; Avérous, L. Progress in Nano-Biocomposites Based on
1144 Polysaccharides and Nanoclays. *Mater. Sci. Eng. R Reports*, **2009**, *67* (1), 1–17.
1145 <https://doi.org/10.1016/j.mser.2009.09.002>.
- 1146 [50] Gao, P.; Wang, F.; Gu, F.; ning, J.; Liang, J.; Li, N.; Ludescher, R. D. Preparation and
1147 Characterization of Zein Thermo-Modified Starch Films. *Carbohydrate Polymers*. **2017**,
1148 pp 1254–1260. <https://doi.org/10.1016/j.carbpol.2016.11.004>.
- 1149 [51] Tatsumi, H.; Katano, H.; Ikeda, T. Kinetic Analysis of Glucoamylase-Catalyzed
1150 Hydrolysis of Starch Granules from Various Botanical Sources. *Biosci. Biotechnol.*
1151 *Biochem.*, **2007**, *71* (4), 946–950. <https://doi.org/10.1271/bbb.60598>.

- 1152 [52] Wang, W.; Wang, Q.; Zhang, Z. Hydrothermal Synthesis of One-Dimensional Assemblies
1153 of Pt Nanoparticles and Their Sensor Application for Simultaneous Determination of
1154 Dopamine and Ascorbic Acid. *J. Nanoparticle Res.*, **2008**, *10* (SUPPL. 1), 255–262.
1155 <https://doi.org/10.1007/s11051-008-9457-1>.
- 1156 [53] Finkenstadt, V. L. Natural Polysaccharides as Electroactive Polymers. *Appl. Microbiol.*
1157 *Biotechnol.*, **2005**, *67* (6), 735–745. <https://doi.org/10.1007/s00253-005-1931-4>.
- 1158 [54] Tester, R. F.; Karkalas, J.; Qi, X. Starch - Composition, Fine Structure and Architecture. *J.*
1159 *Cereal Sci.*, **2004**, *39* (2), 151–165. <https://doi.org/10.1016/j.jcs.2003.12.001>.
- 1160 [55] Jawaheer, S.; White, S. F.; Rughooputh, S. D. D. V.; Cullen, D. C. Enzyme Stabilization
1161 Using Pectin as a Novel Entrapment Matrix in Biosensors. *Anal. Lett.*, **2002**, *35* (13),
1162 2077–2091. <https://doi.org/10.1081/AL-120014997>.
- 1163 [56] Devasenathipathy, R.; Mani, V.; Chen, S. M.; Viswanath, B.; Vasantha, V. S.;
1164 Govindasamy, M. Electrodeposition of Gold Nanoparticles on a Pectin Scaffold and Its
1165 Electrochemical Application in the Selective Determination of Dopamine. *RSC Adv.*, **2014**,
1166 *4* (99), 55900–55907. <https://doi.org/10.1039/c4ra08818b>.
- 1167 [57] Thakur, B.; Amarnath, C. A.; Sawant, S. N. Pectin Coated Polyaniline Nanoparticles for
1168 an Amperometric Glucose Biosensor. *RSC Adv.*, **2014**, *4* (77), 40917–40923.
1169 <https://doi.org/10.1039/c4ra05264a>.
- 1170 [58] Devasenathipathy, R.; Mani, V.; Chen, S. M.; Arulraj, D.; Vasantha, V. S. Highly Stable
1171 and Sensitive Amperometric Sensor for the Determination of Trace Level Hydrazine at
1172 Cross Linked Pectin Stabilized Gold Nanoparticles Decorated Graphene Nanosheets.
1173 *Electrochim. Acta*, **2014**, *135*, 260–269. <https://doi.org/10.1016/j.electacta.2014.05.002>.
- 1174 [59] Mani, V.; Devasenathipathy, R.; Chen, S. M.; Vasantha, V. S.; Ajmal Ali, M.; Huang, S.
1175 T.; Al-Hemaid, F. M. A. A Simple Electrochemical Platform Based on Pectin Stabilized
1176 Gold Nanoparticles for Picomolar Detection of Biologically Toxic Amitrole. *Analyst*,
1177 **2015**, *140* (16), 5764–5771. <https://doi.org/10.1039/c5an00930h>.
- 1178 [60] Noreen, A.; Nazli, Z. i. H.; Akram, J.; Rasul, I.; Mansha, A.; Yaqoob, N.; Iqbal, R.;
1179 Tabasum, S.; Zuber, M.; Zia, K. M. Pectins Functionalized Biomaterials; a New Viable
1180 Approach for Biomedical Applications: A Review. *Int. J. Biol. Macromol.*, **2017**, *101*,
1181 254–272. <https://doi.org/10.1016/j.ijbiomac.2017.03.029>.
- 1182 [61] Alves, G. M.; da Silva, J. L.; Stradiotto, N. R. A Novel Citrus Pectin-Modified Carbon
1183 Paste Electrochemical Sensor Used for Copper Determination in Biofuel. *Measurement:*
1184 *Journal of the International Measurement Confederation*. **2021**, Vol. 169, p 108356.
1185 <https://doi.org/10.1016/j.measurement.2020.108356>.
- 1186 [62] Ridley, B. L.; O'Neill, M. A.; Mohnen, D. Pectins: Structure, Biosynthesis, and
1187 Oligogalacturonide-Related Signaling; **2001**; Vol. 57, pp 929-967.
1188 [https://doi.org/10.1016/S0031-9422\(01\)00113-3](https://doi.org/10.1016/S0031-9422(01)00113-3).
- 1189 [63] Wang, B.; Ji, X.; Zhao, H.; Wang, N.; Li, X.; Ni, R.; Liu, Y. An Amperometric β -Glucan
1190 Biosensor Based on the Immobilization of Bi-Enzyme on Prussian Blue-Chitosan and
1191 Gold Nanoparticles-Chitosan Nanocomposite Films. *Biosens. Bioelectron.*, **2014**, *55*, 113–

- 1192 119. <https://doi.org/10.1016/j.bios.2013.12.004>.
- 1193 [64] Liu, H.; Wang, D.; Song, Z.; Shang, S. Preparation of Silver Nanoparticles on Cellulose
1194 Nanocrystals and the Application in Electrochemical Detection of DNA Hybridization.
1195 *Cellulose*, **2011**, *18* (1), 67–74. <https://doi.org/10.1007/s10570-010-9464-0>.
- 1196 [65] Tiwari, P.; Kumar, A.; Prakash, R. Electrochemical Detection of Azidothymidine on
1197 Modified Probes Based on Chitosan Stabilised Silver Nanoparticles Hybrid Material. *RSC*
1198 *Adv.*, **2015**, *5* (109), 90089–90097. <https://doi.org/10.1039/c5ra15908c>.
- 1199 [66] Tai, M. J. Y.; Perumal, V.; Gopinath, S. C. B.; Raja, P. B.; Ibrahim, M. N. M.; Jantan, I.
1200 N.; Suhaimi, N. S. H.; Liu, W. W. Laser-Scribed Graphene Nanofiber Decorated with Oil
1201 Palm Lignin Capped Silver Nanoparticles: A Green Biosensor. *Sci. Rep.*, **2021**, *11* (1), 1–
1202 9. <https://doi.org/10.1038/s41598-021-85039-2>.
- 1203 [67] de Oliveira, R. D.; Calaça, G. N.; Santos, C. S.; Fujiwara, S. T.; Pessôa, C. A. Preparation,
1204 Characterization and Electrochemistry of Layer-by-Layer Films of Silver Nanoparticles
1205 and Silsesquioxane Polymer. *Colloids Surfaces A Physicochem. Eng. Asp.*, **2016**, *509*,
1206 638–647. <https://doi.org/10.1016/j.colsurfa.2016.09.061>.
- 1207 [68] Dong, L.; Zhang, X.; Ren, S.; Lei, T.; Sun, X.; Qi, Y.; Wu, Q.
1208 Poly(Diallyldimethylammonium Chloride)-Cellulose Nanocrystals Supported Au
1209 Nanoparticles for Nonenzymatic Glucose Sensing. *RSC Adv.*, **2016**, *6* (8), 6436–6442.
1210 <https://doi.org/10.1039/c5ra23935d>.
- 1211 [69] Batra, B.; Pundir, C. S. An Amperometric Glutamate Biosensor Based on Immobilization
1212 of Glutamate Oxidase onto Carboxylated Multiwalled Carbon Nanotubes/Gold
1213 Nanoparticles/Chitosan Composite Film Modified Au Electrode. *Biosens. Bioelectron.*,
1214 **2013**, *47*, 496–501. <https://doi.org/10.1016/j.bios.2013.03.063>.
- 1215 [70] Satyanarayana, M.; Goud, K. Y.; Reddy, K. K.; Gobi, K. V. Biopolymer Stabilized
1216 Nanogold Particles on Carbon Nanotube Support as Sensing Platform for Electrochemical
1217 Detection of 5-Fluorouracil in-Vitro. *Electrochim. Acta*, **2015**, *178*, 608–616.
1218 <https://doi.org/10.1016/j.electacta.2015.08.036>.
- 1219 [71] Ding, L.; Hao, C.; Xue, Y.; Ju, H. A Bio-Inspired Support of Gold Nanoparticles -
1220 Chitosan Nanocomposites Gel for Immobilization and Electrochemical Study of K562
1221 Leukemia Cells. *Biomacromolecules*, **2007**, *8* (4), 1341–1346.
1222 <https://doi.org/10.1021/bm061224y>.
- 1223 [72] Jodar, L. V.; Santos, F. A.; Zucolotto, V.; Janegitz, B. C. Electrochemical Sensor for
1224 Estriol Hormone Detection in Biological and Environmental Samples. *J. Solid State*
1225 *Electrochem.*, **2018**, *22* (5), 1431–1438. <https://doi.org/10.1007/s10008-017-3726-9>.
- 1226 [73] Devasenathipathy, R.; Karuppiyah, C.; Chen, S. M.; Mani, V.; Vasantha, V. S.; Ramaraj, S.
1227 Highly Selective Determination of Cysteine Using a Composite Prepared from
1228 Multiwalled Carbon Nanotubes and Gold Nanoparticles Stabilized with Calcium
1229 Crosslinked Pectin. *Microchim. Acta*, **2015**, *182* (3–4), 727–735.
1230 <https://doi.org/10.1007/s00604-014-1380-9>.
- 1231 [74] Shahrokhian, S.; Balotf, H.; Ghalkhani, M. Nano Composite Coating Based on Cellulose

- 1232 Nanofibers/Carbon Nanoparticles: Application to Voltammetric Determination of
 1233 Clonazepam. *J. Solid State Electrochem.*, **2015**, *19* (1), 251–260.
 1234 <https://doi.org/10.1007/s10008-014-2597-6>.
- 1235 [75] Sarkar, T.; Bohidar, H. B.; Solanki, P. R. Carbon Dots-Modified Chitosan Based
 1236 Electrochemical Biosensing Platform for Detection of Vitamin D. *International Journal of*
 1237 *Biological Macromolecules*. **2018**, Vol. *109*, pp 687–697.
 1238 <https://doi.org/10.1016/j.ijbiomac.2017.12.122>.
- 1239 [76] Yazhini, K.; Suja, S. K.; G., J. K.; Bagyalaksmi, J.; Pavalamalar, S. Non-Enzymatic
 1240 Sensing of Kidney Dysfunction Biomarker Using Pectin – MWCNT Nanocomposite.
 1241 *Appl. Surf. Sci.*, **2018**, *449*, 736–744. <https://doi.org/10.1016/j.apsusc.2018.01.197>.
- 1242 [77] Duran, G. M.; Benavidez, T. E.; Giuliani, J. G.; Rios, A.; Garcia, C. D. Synthesis of
 1243 CuNP-Modified Carbon Electrodes Obtained by Pyrolysis of Paper. *Sensors Actuators, B*
 1244 *Chem.*, **2016**, *227*, 626–633. <https://doi.org/10.1016/j.snb.2015.12.093>.
- 1245 [78] Wang, Y.; Wei, W.; Zeng, J.; Liu, X.; Zeng, X. Fabrication of a Copper
 1246 Nanoparticle/Chitosan/Carbon Nanotube-Modified Glassy Carbon Electrode for
 1247 Electrochemical Sensing of Hydrogen Peroxide and Glucose. *Microchim. Acta*, **2008**, *160*
 1248 (1–2), 253–260. <https://doi.org/10.1007/s00604-007-0844-6>.
- 1249 [79] Chen, T. W.; Chinnapaiyan, S.; Chen, S. M.; Ajmal Ali, M.; Elshikh, M. S.; Hossam
 1250 Mahmoud, A. Facile Synthesis of Copper Ferrite Nanoparticles with Chitosan Composite
 1251 for High-Performance Electrochemical Sensor. *Ultrason. Sonochem.*, **2020**, *63* (October
 1252 2019), 104902. <https://doi.org/10.1016/j.ultsonch.2019.104902>.
- 1253 [80] Chokkareddy, R.; Redhi, G. G.; Karthick, T. A Lignin Polymer Nanocomposite Based
 1254 Electrochemical Sensor for the Sensitive Detection of Chlorogenic Acid in Coffee
 1255 Samples. *Heliyon*. **2019**, Vol. *5*. <https://doi.org/10.1016/j.heliyon.2019.e01457>.
- 1256 [81] Capecchi, E.; Piccinino, D.; Tomaino, E.; Bizzarri, B. M.; Polli, F.; Antiochia, R.; Mazzei,
 1257 F.; Saladino, R. Lignin Nanoparticles Are Renewable and Functional Platforms for the
 1258 Concanavalin a Oriented Immobilization of Glucose Oxidase-Peroxidase in Cascade Bio-
 1259 Sensing. *RSC Adv.*, **2020**, *10* (48), 29031–29042. <https://doi.org/10.1039/d0ra04485g>.
- 1260 [82] Mani, V.; Devasenathipathy, R.; Chen, S. M.; Wang, S. F.; Devi, P.; Tai, Y.
 1261 Electrodeposition of Copper Nanoparticles Using Pectin Scaffold at Graphene Nanosheets
 1262 for Electrochemical Sensing of Glucose and Hydrogen Peroxide. *Electrochim. Acta*, **2015**,
 1263 *176*, 804–810. <https://doi.org/10.1016/j.electacta.2015.07.098>.
- 1264 [83] Ranjbar, S.; Shahrokhian, S. Design and Fabrication of an Electrochemical Aptasensor
 1265 Using Au Nanoparticles/Carbon Nanoparticles/Cellulose Nanofibers Nanocomposite for
 1266 Rapid and Sensitive Detection of Staphylococcus Aureus. *Bioelectrochemistry*. **2018**, Vol.
 1267 *123*, pp 70–76. <https://doi.org/10.1016/j.bioelechem.2018.04.018>.
- 1268 [84] Darvishi, E.; Ehzari, H.; Shahlaei, M.; Behbood, L.; Arkan, E. The Electrochemical
 1269 Immunosensor for Detection of Prostatic Specific Antigen Using Quince Seed Mucilage-
 1270 GNPs-SNPs as a Green Composite. *Bioelectrochemistry*. **2021**, Vol. *139*, p 107744.
 1271 <https://doi.org/10.1016/j.bioelechem.2021.107744>.

- 1272 [85] Jagadish, R.; Yellappa, S.; Mahanthappa, M.; Chandrasekhar, K. B. Zinc Oxide
1273 Nanoparticle-Modified Glassy Carbon Electrode as a Highly Sensitive Electrochemical
1274 Sensor for the Detection of Caffeine. *J. Chinese Chem. Soc.*, **2017**, *64* (7), 813–821.
1275 <https://doi.org/10.1002/jccs.201600817>.
- 1276 [86] Jagadish, R.; Mahanthappa, M.; Yellappa, S.; Chandrasekhar, K. B. γ -Fe₂O₃
1277 Nanoparticles Modified Glassy Carbon Electrode for the Sensitive Detection of Folic
1278 Acid. *Mater. Res. Express*, **2019**, *6*, 0–18. <https://doi.org/10.1088/2053-1591/ab3bba>.
- 1279 [87] Mulyasuryani, A.; Tjahjanto, R. T.; Andawiyah, R. Simultaneous Voltammetric Detection
1280 of Acetaminophen and Caffeine Base on Cassava Starch-Fe₃O₄ Nanoparticles Modified
1281 Glassy Carbon Electrode. *Chemosensors*, **2019**, *7* (4).
1282 <https://doi.org/10.3390/chemosensors7040049>.
- 1283 [88] Arévalo, F. J.; Osuna-Sánchez, Y.; Sandoval-Cortés, J.; Di Tocco, A.; Granero, A. M.;
1284 Robledo, S. N.; Zon, M. A.; Vettorazzi, N. R.; Martínez, J. L.; Segura, E. P.; et al.
1285 Development of an Electrochemical Sensor for the Determination of Glycerol Based on
1286 Glassy Carbon Electrodes Modified with a Copper Oxide Nanoparticles/Multiwalled
1287 Carbon Nanotubes/Pectin Composite. *Sensors and Actuators, B: Chemical*. **2017**, Vol.
1288 *244*, pp 949–957. <https://doi.org/10.1016/j.snb.2017.01.093>.
- 1289 [89] Tortolini, C.; Capecchi, E.; Tasca, F.; Pofi, R.; Venneri, M. A.; Saladino, R.; Antiochia, R.
1290 Novel Nanoarchitectures Based on Lignin Nanoparticles for Electrochemical Eco-friendly
1291 Biosensing Development. *Nanomaterials*, **2021**, *11* (3), 1–17.
1292 <https://doi.org/10.3390/nano11030718>.
- 1293 [90] Melissa A. L. Nikolic´, K. D. and P. J. H. Chapter 16 Biodegradation and Applications of
1294 Nanobiocomposites; **2012**; Vol. 50. <https://doi.org/10.1007/978-1-4471-4108-2>.
- 1295 [91] Das, S.; Saha, M. Potato Starch-Derived Almond-Shaped Carbon Nanoparticles for Non
1296 Enzymatic Detection of Sucrose. *Xinxing Tan Cailiao/New Carbon Mater.*, **2015**, *30* (3),
1297 244–251. [https://doi.org/10.1016/S1872-5805\(15\)60189-5](https://doi.org/10.1016/S1872-5805(15)60189-5).
- 1298 [92] Lin, Q.; Peng, X.; Zhang, Z. Electrochemical Determination of Hg(II) Ions Based on
1299 Biosynthesized Spherical Activated Carbon from Potato Starch. *Int. J. Electrochem. Sci.*,
1300 **2017**, *12* (3), 2232–2241. <https://doi.org/10.20964/2017.03.08>.
- 1301 [93] Gautam, V.; Singh, K. P.; Yadav, V. L. Preparation and Characterization of Green-Nano-
1302 Composite Material Based on Polyaniline, Multiwalled Carbon Nano Tubes and
1303 Carboxymethyl Cellulose: For Electrochemical Sensor Applications. *Carbohydr. Polym.*,
1304 **2018**, *189* (October 2017), 218–228. <https://doi.org/10.1016/j.carbpol.2018.02.029>.
- 1305 [94] Lakard, B.; Magnin, D.; Deschaume, O.; Vanlancker, G.; Glinel, K.; Demoustier-
1306 Champagne, S.; Nysten, B.; Jonas, A. M.; Bertrand, P.; Yunus, S. Urea Potentiometric
1307 Enzymatic Biosensor Based on Charged Biopolymers and Electrodeposited Polyaniline.
1308 *Biosensors and Bioelectronics*. **2011**, Vol. 26, pp 4139–4145.
1309 <https://doi.org/10.1016/j.bios.2011.04.009>.
- 1310 [95] Kushwaha, C. S.; Singh, P.; Abbas, N. S.; Shukla, S. K. Self-Activating Zinc Oxide
1311 Encapsulated Polyaniline-Grafted Chitosan Composite for Potentiometric Urea Sensor. *J.*
1312 *Mater. Sci. Mater. Electron.*, **2020**, *31* (14), 11887–11896.

- 1313 <https://doi.org/10.1007/s10854-020-03743-7>.
- 1314 [96] Gautam, V.; Singh, K. P.; Yadav, V. L. Polyaniline/MWCNTs/Starch Modified Carbon
1315 Paste Electrode for Non-Enzymatic Detection of Cholesterol: Application to Real Sample
1316 (Cow Milk). *Anal. Bioanal. Chem.*, **2018**, *410* (8), 2173–2181.
1317 <https://doi.org/10.1007/s00216-018-0880-6>.
- 1318 [97] Gautam, V.; Singh, K. P.; Yadav, V. L. Polyaniline/Multiwall Carbon Nanotubes/Starch
1319 Nanocomposite Material and Hemoglobin Modified Carbon Paste Electrode for Hydrogen
1320 Peroxide and Glucose Biosensing. *Int. J. Biol. Macromol.*, **2018**, *111*, 1124–1132.
1321 <https://doi.org/10.1016/j.ijbiomac.2018.01.094>.
- 1322 [98] Uzunçar, S.; Özdoğan, N.; Ak, M. Amperometric Detection of Glucose and H₂O₂ Using
1323 Peroxide Selective Electrode Based on Carboxymethylcellulose/Polypyrrole and Prussian
1324 Blue Nanocomposite. *Mater. Today Commun.*, **2020**, *26* (October 2020).
1325 <https://doi.org/10.1016/j.mtcomm.2020.101839>.
- 1326 [99] Dervisevic, M.; Dervisevic, E.; Çevik, E.; Şenel, M. Novel Electrochemical Xanthine
1327 Biosensor Based on Chitosan–Polypyrrole–Gold Nanoparticles Hybrid Bio-
1328 Nanocomposite Platform. *Journal of Food and Drug Analysis*. **2017**, Vol. 25, pp 510–519.
1329 <https://doi.org/10.1016/j.jfda.2016.12.005>.
- 1330 [100] Abdul Amir AL-Mokaram, A. M. A.; Yahya, R.; Abdi, M. M.; Muhammad Ekramul
1331 Mahmud, H. N. One-Step Electrochemical Deposition of Polypyrrole–Chitosan–Iron
1332 Oxide Nanocomposite Films for Non-Enzymatic Glucose Biosensor. *Materials Letters*.
1333 **2016**, Vol. 183, pp 90–93. <https://doi.org/10.1016/j.matlet.2016.07.049>.
- 1334 [101] Arulraj, A. D.; Devasenathipathy, R.; Chen, S. M.; Vasantha, V. S.; Wang, S. F.
1335 Femtomolar Detection of Mercuric Ions Using Polypyrrole, Pectin and Graphene
1336 Nanocomposites Modified Electrode. *J. Colloid Interface Sci.*, **2016**, *483*, 268–274.
1337 <https://doi.org/10.1016/j.jcis.2016.08.026>.
- 1338 [102] Vijaya, N.; Selvasekarapandian, S.; Sornalatha, M.; Sujithra, K. S.; Monisha, S. Proton-
1339 Conducting Biopolymer Electrolytes Based on Pectin Doped with NH₄X (X=Cl, Br).
1340 *Ionics (Kiel)*, **2017**, *23* (10), 2799–2808. <https://doi.org/10.1007/s11581-016-1852-5>.
- 1341 [103] Zhang, Z.; Zhang, J.; Zhang, H.; Xu, J.; Wen, Y.; Ding, W. Characterization of
1342 PEDOT:PSS-Reduced Graphene Oxide@Pd Composite Electrode and Its Application in
1343 Voltammetric Determination of Vitamin K₃. *J. Electroanal. Chem.*, **2016**, *775*, 258–266.
1344 <https://doi.org/10.1016/j.jelechem.2016.06.005>.
- 1345 [104] Xu, G.; Liang, S.; Zhang, M.; Fan, J.; Feng, J.; Yu, X. Studies on the Electrochemical and
1346 Dopamine Sensing Properties of AgNP-Modified Carboxylated Cellulose Nanocrystal-
1347 Doped Poly(3,4-Ethylenedioxythiophene). *Ionics (Kiel)*, **2017**, *23* (11), 3211–3218.
1348 <https://doi.org/10.1007/s11581-017-2112-z>.
- 1349 [105] Xu, G.; Zhang, M.; Yu, X. Electrochemical Detection of Nitrite in Food Based on Poly
1350 (3,4-Ethylenedioxythiophene) Doped with Fe₃O₄ Nanoparticles Loaded Carboxylated
1351 Nanocrystalline Cellulose. *Acta Chim. Slov.*, **2018**, *65* (3), 502–511.
1352 <https://doi.org/10.17344/acsi.2017.3974>.

- 1353 [106] Baker, D. A.; Rials, T. G. Recent Advances in Low-Cost Carbon Fiber Manufacture from
1354 Lignin. *J. Appl. Polym. Sci.*, **2013**, *130* (2), 713–728. <https://doi.org/10.1002/app.39273>.
- 1355 [107] Demiroğlu Mustafov, S.; Mohanty, A. K.; Misra, M.; Seydibeyoğlu, M. Ö. Fabrication of
1356 Conductive Lignin/PAN Carbon Nanofiber with Enhanced Graphene for the Modified
1357 Electrode. *Carbon N. Y.*, **2019**, *147*, 262–275.
1358 <https://doi.org/10.1016/j.carbon.2019.02.058>.
- 1359 [108] Gonzalez-Vogel, A.; Fogde, A.; Crestini, C.; Sandberg, T.; Huynh, T. P.; Bobacka, J.
1360 Molecularly Imprinted Conducting Polymer for Determination of a Condensed Lignin
1361 Marker. *Sensors Actuators, B Chem.*, **2019**, *295* (March), 186–193.
1362 <https://doi.org/10.1016/j.snb.2019.05.011>.
- 1363 [109] F. Graça, M. P.; Rudnitskaya, A.; Fernando, F. A.; Evtuguin, D. V.; Maria, M. T.; Joaõ, J.
1364 A.; C. Costa, L. Electrochemical Impedance Study of the Lignin-Derived Conducting
1365 Polymer. *Electrochim. Acta*, **2012**, *76*, 69–76.
1366 <https://doi.org/10.1016/j.electacta.2012.04.155>.
- 1367 [110] Gonçalves, S. S. L.; Rudnitskaya, A.; Sales, A. J. M.; Costa, L. M. C.; Evtuguin, D. V.
1368 Nanocomposite Polymeric Materials Based on Eucalyptus Lignoboost® Kraft Lignin for
1369 Liquid Sensing Applications. *Materials (Basel)*, **2020**, *13* (7).
1370 <https://doi.org/10.3390/ma13071637>.
- 1371 [111] Rudnitskaya, A.; Evtuguin, D. V.; Costa, L. C.; Pedro Graça, M. P.; Fernandes, A. J. S.;
1372 Rosario Correia, M.; Teresa Gomes, M. T.; Oliveira, J. A. B. P. Potentiometric Chemical
1373 Sensors from Lignin-Poly(Propylene Oxide) Copolymers Doped by Carbon Nanotubes.
1374 *Analyst*, **2013**, *138* (2), 501–508. <https://doi.org/10.1039/c2an36390a>.
- 1375 [112] Palanisamy, S.; Velusamy, V.; Balu, S.; Velmurugan, S.; Yang, T. C. K.; Chen, S. W.
1376 Sonochemical Synthesis and Anchoring of Zinc Oxide on Hemin-Mediated Multiwalled
1377 Carbon Nanotubes-Cellulose Nanocomposite for Ultra-Sensitive Biosensing of H₂O₂.
1378 *Ultrasonics Sonochemistry*. **2020**, Vol. *63*, p 104917.
1379 <https://doi.org/10.1016/j.ultsonch.2019.104917>.
- 1380 [113] Zaid, M. H. M.; Che-Engku-Chik, C. E. N.; Yusof, N. A.; Abdullah, J.; Othman, S. S.;
1381 Issa, R.; Md Noh, M. F.; Wasoh, H. DNA Electrochemical Biosensor Based on Iron
1382 Oxide/Nanocellulose Crystalline Composite Modified Screen-Printed Carbon Electrode
1383 for Detection of Mycobacterium Tuberculosis. *Molecules*, **2020**, *25* (15).
1384 <https://doi.org/10.3390/molecules25153373>.
- 1385 [114] Khalilzadeh, M. A.; Tajik, S.; Beitollahi, H.; Venditti, R. A. Green Synthesis of Magnetic
1386 Nanocomposite with Iron Oxide Deposited on Cellulose Nanocrystals with Copper
1387 (Fe₃O₄@CNC/Cu): Investigation of Catalytic Activity for the Development of a
1388 Venlafaxine Electrochemical Sensor. *Ind. Eng. Chem. Res.*, **2020**, *59* (10), 4219–4228.
1389 <https://doi.org/10.1021/acs.iecr.9b06214>.
- 1390 [115] Singh, J.; Srivastava, M.; Kalita, P.; Malhotra, B. D. A Novel Ternary
1391 NiFe₂O₄/CuO/FeO-Chitosan Nanocomposite as a Cholesterol Biosensor. *Process*
1392 *Biochem.*, **2012**, *47* (12), 2189–2198. <https://doi.org/10.1016/j.procbio.2012.08.012>.
- 1393 [116] Yazhini, K.; Suja, S. K. Synthesis and Characterization of Hetero-Metal Oxide Nano-

- 1394 Hybrid Composite on Pectin Scaffold. *Appl. Surf. Sci.*, **2019**, *491* (February), 195–205.
1395 <https://doi.org/10.1016/j.apsusc.2019.06.150>.
- 1396 [117] Liu, L.; Yang, M.; Zhao, H.; Xu, Y.; Cheng, X.; Zhang, X.; Gao, S.; Song, H.; Huo, L. Co
1397 3 O 4 /Carbon Hollow Nanospheres for Resistive Monitoring of Gaseous Hydrogen
1398 Sulfide and for Nonenzymatic Amperometric Sensing of Dissolved Hydrogen Peroxide.
1399 *Microchim. Acta*, **2019**, *186* (3), 4–13. <https://doi.org/10.1007/s00604-019-3253-8>.
- 1400 [118] Barsan, M. M.; David, M.; Florescu, M.; Țugulea, L.; Brett, C. M. A. A New Self-
1401 Assembled Layer-by-Layer Glucose Biosensor Based on Chitosan Biopolymer Entrapped
1402 Enzyme with Nitrogen Doped Graphene. *Bioelectrochemistry*, **2014**, *99*, 46–52.
1403 <https://doi.org/10.1016/j.bioelechem.2014.06.004>.
- 1404 [119] Adumitrăchioaie, A.; Tertiș, M.; Suci, M.; Graur, F.; Cristea, C. A Novel
1405 Immunosensing Platform for Serotonin Detection in Complex Real Samples Based on
1406 Graphene Oxide and Chitosan. *Electrochimica Acta*. **2019**, Vol. *311*, pp 50–61.
1407 <https://doi.org/10.1016/j.electacta.2019.04.128>.
- 1408 [120] Poletti, F.; Favaretto, L.; Kovtun, A.; Treossi, E.; Corticelli, F.; Gazzano, M.; Palermo, V.;
1409 Zanardi, C.; Melucci, M. Electrochemical Sensing of Glucose by Chitosan Modified
1410 Graphene Oxide. *J. Phys. Mater.*, **2020**, *3* (1), 014011. <https://doi.org/10.1088/2515-7639/ab5e51>.
1411
- 1412 [121] Zhou, J.; Li, S.; Noroozifar, M.; Kerman, K. Graphene Oxide Nanoribbons in Chitosan for
1413 Simultaneous Electrochemical Detection of Guanine, Adenine, Thymine and Cytosine.
1414 *Biosensors*, **2020**, *10* (4). <https://doi.org/10.3390/bios10040030>.
- 1415 [122] Krishna, R.; Campiña, J. M.; Fernandes, P. M. V.; Ventura, J.; Titus, E.; Silva, A. F.
1416 Reduced Graphene Oxide-Nickel Nanoparticles/Biopolymer Composite Films for the Sub-
1417 Millimolar Detection of Glucose. *Analyst*, **2016**, *141* (13), 4151–4161.
1418 <https://doi.org/10.1039/c6an00475j>.
- 1419 [123] Orzari, L. O.; Santos, F. A.; Janegitz, B. C. Manioc Starch Thin Film as Support of
1420 Reduced Graphene Oxide: A Novel Architecture for Electrochemical Sensors. *J.*
1421 *Electroanal. Chem.*, **2018**, *823* (January), 350–358.
1422 <https://doi.org/10.1016/j.jelechem.2018.06.036>.
- 1423 [124] Kasturi, P. R.; Aparna, T. K.; Arokiyanathan, A. L.; Lakshmi pathi, S.; Sivasubramanian,
1424 R.; Lee, Y. S.; Selvan, R. K. Synthesis of Metal-Free Nitrogen-Enriched Porous Carbon
1425 and Its Electrochemical Sensing Behavior for the Highly Sensitive Detection of
1426 Dopamine: Both Experimental and Theoretical Investigation. *Mater. Chem. Phys.*, **2021**,
1427 *260* (November 2020), 124094. <https://doi.org/10.1016/j.matchemphys.2020.124094>.
- 1428 [125] Kokulnathan, T.; Ramaraj, S.; Chen, S.-M.; Han-Yu, Y. Eco-Friendly Synthesis of
1429 Biocompatible Pectin Stabilized Graphene Nanosheets Hydrogel and Their Application
1430 for the Simultaneous Electrochemical Determination of Dopamine and Paracetamol in
1431 Real Samples. *J. Electrochem. Soc.*, **2018**, *165* (5), B240–B249.
1432 <https://doi.org/10.1149/2.0011807jes>.
- 1433 [126] Wang, H.; Wen, F.; Chen, Y.; Sun, T.; Meng, Y.; Zhang, Y. Electrocatalytic
1434 Determination of Nitrite Based on Straw Cellulose/Molybdenum Sulfide Nanocomposite.

- 1435 *Biosens. Bioelectron.*, **2016**, 85, 692–697. <https://doi.org/10.1016/j.bios.2016.05.078>.
- 1436 [127] Zhang, Y.; Wen, F.; Huang, Z.; Tan, J.; Zhou, Z.; Yuan, K.; Wang, H. Nitrogen Doped
1437 Lignocellulose/Binary Metal Sulfide Modified Electrode: Preparation and Application for
1438 Non-Enzymatic Ascorbic Acid, Dopamine and Nitrite Sensing. *J. Electroanal. Chem.*,
1439 **2017**, 806 (July), 150–157. <https://doi.org/10.1016/j.jelechem.2017.10.066>.
- 1440 [128] Camargo, J. R.; Baccarin, M.; Raymundo-Pereira, P. A.; Campos, A. M.; Oliveira, G. G.;
1441 Fatibello-Filho, O.; Oliveira, O. N.; Janegitz, B. C. Electrochemical Biosensor Made with
1442 Tyrosinase Immobilized in a Matrix of Nanodiamonds and Potato Starch for Detecting
1443 Phenolic Compounds. *Anal. Chim. Acta*, **2018**, 1034, 137–143.
1444 <https://doi.org/10.1016/j.aca.2018.06.001>.
- 1445 [129] Zambianco, N. A.; Silva, T. A.; Zanin, H.; Fatibello-Filho, O.; Janegitz, B. C. Novel
1446 Electrochemical Sensor Based on Nanodiamonds and Manioc Starch for Detection of
1447 Diquat in Environmental Samples. *Diamond and Related Materials*. **2019**, Vol. 98, p
1448 107512. <https://doi.org/10.1016/j.diamond.2019.107512>.
- 1449 [130] Fernandes-Junior, W. S.; Zaccarin, L. F.; Oliveira, G. G.; De Oliveira, P. R.; Kalinke, C.;
1450 Bonacin, J. A.; Prakash, J.; Janegitz, B. C. Electrochemical Sensor Based on
1451 Nanodiamonds and Manioc Starch for Detection of Tetracycline. *J. Sensors*, **2021**, Vol.
1452 2021, p 6622612. <https://doi.org/10.1155/2021/6622612>.

1453

1454 **Acknowledgements**

1455 Thanking note to Minister of Higher Education Malaysia for supporting the research with
1456 Fundamental Research Grant Scheme (FRGS) (FRGS/1/2020/TKO/UTP/03/7) and Universiti
1457 Teknologi PETRONAS (UTP) for giving chance to carry out the research in Nanotechnology
1458 Research Laboratory and Dye Solar Cell Laboratory.

1459